

COMPARISON OF THE FLAW DETECTION ABILITIES OF PHASED ARRAY
AND CONVENTIONAL ULTRASONIC TESTING METHODS IN VARIOUS
STEELS

A THESIS SUBMITTED TO
THE GRADUATE SCHOOL OF NATURAL AND APPLIED SCIENCES
OF
MIDDLE EAST TECHNICAL UNIVERSITY

BY

MURAT YALÇIN

IN PARTIAL FULFILLMENT OF THE REQUIREMENTS
FOR
THE DEGREE OF MASTER OF SCIENCE
IN
METALLURGICAL AND MATERIALS ENGINEERING

SEPTEMBER 2014

Approval of the thesis:

**COMPARISON OF THE FLAW DETECTION ABILITIES OF PHASED
ARRAY AND CONVENTIONAL ULTRASONIC TESTING METHODS IN
VARIOUS STEELS**

Submitted by **MURAT YALÇIN** in partial fulfillment of the requirements for the degree of **Master of Science in Metallurgical and Materials Engineering Department, Middle East Technical University** by,

Prof. Dr. Canan Özgen
Dean, Graduate School of **Natural and Applied Sciences** _____

Prof. Dr. C. Hakan Gür
Head of Department, **Metallurgical and Materials Engineering** _____

Prof. Dr. C. Hakan Gür
Supervisor, **Metallurgical and Materials Eng. Dept., METU** _____

Examining Committee Members:

Prof. Dr. Tayfur Öztürk
Metallurgical and Materials Engineering Dept., METU _____

Prof. Dr. C. Hakan Gür
Metallurgical and Materials Engineering Dept., METU _____

Prof. Dr. A. Bülent Doyum
Mechanical Engineering Dept., METU _____

Assoc. Prof. Dr. Arcan F. Dericioğlu
Metallurgical and Materials Engineering Dept., METU _____

Assist. Prof. Dr. Mert Efe
Metallurgical and Materials Engineering Dept., METU _____

Date: 08.09.2014

I hereby declare that all information in this document has been obtained and presented in accordance with academic rules and ethical conduct. I also declare that, as required by these rules and conduct, I have fully cited and referenced all material and results that are not original to this work.

Name, Last name: Murat YALÇIN

Signature:

ABSTRACT

COMPARISON OF THE FLAW DETECTION ABILITIES OF PHASED ARRAY AND CONVENTIONAL ULTRASONIC TESTING METHODS IN VARIOUS STEELS

YALÇIN, Murat

M.S., Department of Metallurgical and Materials Engineering

Supervisor: Prof. Dr. C. Hakan GÜR

September 2014, 84 pages

Applications of Non – Destructive Testing (NDT) are very broad varying from the medical to heavy industries. Several advanced NDT methods, mainly developed form of the conventional methods, are used to render the technique more flexible and easier to interpret. Ultrasonic Phased Array method can be employed in almost any test, where conventional Ultrasonic Testing (UT) has traditionally been used. The benefits of Phased Array technology over conventional UT come from its ability to use multiple elements to steer, focus and scan beams with a single transducer assembly. In this study, the advantages and limitations of the Phased Array system will be investigated via using several test blocks, prepared from different types of steels, having well-defined artificial defects. The reliability of the Phased Array and conventional Ultrasonic Testing methods will be compared using a statistical approach, the Probability of Detection (PoD).

Keywords: Ultrasonic Testing; Phased Array; Probability of Detection (PoD).

ÖZ

ÇEŞİTLİ ÇELİKLERDE FAZ DİZİSİ VE GELENEKSEL ULTRASONİK TEST METOTLARININ HATA TESPİT KABİLİYETLERİNİN KARŞILAŞTIRILMASI

YALÇIN, Murat

Yüksek Lisans, Metalurji ve Malzeme Mühendisliği Bölümü

Tez Yöneticisi: Prof. Dr. C. Hakan GÜR

Eylül 2014, 84 sayfa

Tahribatsız muayene tıptan ağır sanayiye kadar geniş uygulama alanına sahiptir. Geleneksel tahribatsız muayene metotları, sürekli geliştirilerek daha esnek ve kolay yorumlanabilir hale getirilmektedir. Ultrasonik metodun geliştirilmiş hali olan Faz Dizisi (PA: Phased Array) metodu konvansiyonel ultrasonik testin kullanıldığı hemen her alanda kullanılabilir. PA teknolojisinin avantajı, tek bir transdüser sistemi içinde çok sayıda küçük transdüserin faz farkı ile tetiklenip ultrasonik dalgaların kontrollü olarak farklı açılarda ve farklı mesafelerde odaklanarak muayene edilecek parçanın tamamen taranabilmesidir. Bu çalışmada, çeşitli yapay hatalara sahip ve farklı çeliklerden hazırlanan test blokları kullanılarak PA sisteminin geleneksel ultrasonik yöntemle göre avantajları ve sınırlamaları araştırılmıştır. Bu amaçla, istatistiksel bir yöntem olan Hata Tespit Olasılığı (PoD: Probability of Detection) yöntemi kullanılmıştır.

Anahtar Sözcükler: Ultrasonik Test; Faz Dizisi; Hata Tespit Olasılığı (PoD).

To my dear family

ACKNOWLEDGEMENTS

There are a number of people without whom this thesis might not have been written, and to whom I am greatly indebted.

Firstly and most importantly, I would like to express my deepest gratitude to my supervisor, Prof. Dr. C. Hakan Gür for his guidance, endless support, encouragement and great wisdom during my thesis studies.

Secondly, I am very thankful to H. İlker Yelbay for his continuous help through my laboratory studies.

Moreover, I would like to thank warmly to my dear friends, Özgün Başkan Taştan, Erhan Turgut and especially Aylin Güneş, for their moral support and friendship during my master's education.

I am also thankful to all staff of the METU Welding Technology and Non – Destructive Testing Research / Application Center for their helps and supports.

Finally, I would like to express my special thanks to my parents Sunay Yalçın , Ertuğrul Yalçın, my brother Fırat Yalçın for their infinite support during my whole life.

The last but not the least, I owe a debt of gratitude to my wife Gözde Yalçın for her endless love, moral and encouragement which have let me to start and finish my thesis studies and lastly, words cannot express how grateful I am to my son Arda Deniz Yalçın who is the inspiration of my life.

TABLE OF CONTENTS

ABSTRACT.....	v
ÖZ.....	vi
ACKNOWLEDGEMENTS.....	viii
TABLE OF CONTENTS.....	ix
LIST OF FIGURES.....	xiii
LIST OF TABLES.....	xvi
1 INTRODUCTION.....	1
1.1 GENERAL.....	1
1.2 ULTRASONIC TESTING.....	3
1.2.1 History and Introduction of Ultrasonic.....	3
1.2.2 Advantages & Disadvantages of Ultrasonic Testing.....	4
1.2.3 Theory of Ultrasonic Testing.....	5
1.2.4 Attenuation of Sound Waves.....	6
1.2.5 Ultrasonic Equipment and Transducers.....	8
1.2.5.1 Piezoelectric transducers.....	8
1.2.5.2 The characteristics of Piezoelectric Transducers.....	9
1.2.5.3 The characteristics of Piezoelectric Transducers Beams.....	10
1.2.5.4 Other Ultrasonic Equipments.....	12
1.2.6 Ultrasonic Measurement Systems.....	13
1.2.6.1 The Transmission Method.....	13
1.2.6.2 The Pulse – Echo System.....	14

1.2.7	Data Presentation of Ultrasonic Testing.....	15
1.2.7.1	A – Scan Presentation	15
1.2.7.2	B – Scan Presentation.....	16
1.2.7.3	C – Scan Presentation.....	17
1.2.7.4	S – Scan Presentation	17
1.3	PHASED ARRAY SYSTEM.....	18
1.3.1	General Introduction and History of Phased Array System.....	18
1.3.2	Basic Principles of Phased Array	19
1.3.3	Advantages of Phased Array against Conventional UT.....	27
1.3.4	Applications of Phased Array System.....	28
1.4	Probability of Detection (PoD)	29
1.4.1	Introduction and History of Probability of Detection (PoD).....	29
1.4.2	Usage of Probability of Detection Data	31
1.4.3	PoD (a) Curves from Hit / Miss Data	32
1.4.4	PoD (a) Curves from Signal Response Data (\hat{a})	35
1.4.5	Parameters Affecting Probability of Detection	37
2	EXPERIMENTAL PROCEDURE	43
2.1	Material Selection and Properties	43
2.2	Sample Preparation	46
2.2.1	Specimen Type 1	47
2.2.2	Specimen Type 2.....	48
2.3	Metallographic Investigations	51
2.4	Ultrasonic Inspections	52
2.5	Phased Array Inspections	55
2.6	Probability of Detection Analysis	57

3	RESULTS & DISCUSSION	59
3.1	a vs \hat{a} Model Selection for PoD Analysis	59
3.1.1	a vs \hat{a} Models for Type 1 Specimen.....	59
3.1.2	a vs \hat{a} Models for Type 2 Specimen.....	60
3.2	a vs \hat{a} Linear Model Determination for PoD Analysis	63
3.2.1	a vs \hat{a} Linear Model for Type 1 Specimen	64
3.2.2	a vs \hat{a} Linear Model for Type 2 Specimen.....	66
3.3	Type 1 Specimen PoD Analysis.....	70
3.4	Type 2 Specimen PoD Analysis.....	72
3.4.1	Type 2 Specimen (St-37) PoD Analysis.....	72
3.4.2	Type 2 Specimen (SAE 4140) PoD Analysis.....	73
3.4.3	Type 2 Specimen (SAE 316 L) PoD Analysis.....	75
4	CONCLUSION.....	79
	REFERENCES.....	81

LIST OF FIGURES

FIGURES

Figure 1.1 Frequency ranges of ultrasound in different applications [1].	3
Figure 1.2 The illustrations of longitudinal and transverse waves.	6
Figure 1.3 Variation of apparent attenuation with respect to amount of nodular graphite [5].	8
Figure 1.4 (a) Variations of acoustic sound pressure with distance ratio for circular crystal. (b) Schematic sound field.	11
Figure 1.5 Schematic views of ultrasonic beam spread and divergence	12
Figure 1.6 Dead zone in pulse – echo system (left) and overlapping echoes from multiple reflections.	15
Figure 1.7 Typical A-Scan presentation [7].	16
Figure 1.8 Typical B – Scan presentation [7].	16
Figure 1.9 Direction of motion and C-scan image showing the reflectors (holes) position [7].	17
Figure 1.10 Zero degree wedge, longitudinal waves $-30 - +30^\circ$ S-scan image (left), Shear waves in the refracted angle between $+35 - +70^\circ$ S-scan image (right) [7].	18
Figure 1.11 Different shaped and wedged phased array probes	20
Figure 1.12 Multiangle scans and probe movement requirement on monocrystal inspection (left), Focused beam through required region without probe movement on linear array probe (right) [10].	20

Figure 1.13 Focusing control and beam sweeping using time delays of multiple elements [11].	21
Figure 1.14 Detection of misoriented cracks by monocrystal (left) and multielement probes (right) [12].	23
Figure 1.15 Beam forming and time delay for pulsing and receiving multiple beams [12].	24
Figure 1.16 Beam focusing principle for normal (a),and angled (b) incidences [10].	25
Figure 1.17 Electronic scanning with normal beam (virtual probe aperture=16 elements) [12].	25
Figure 1.18 Detection a group of cracks in volume corrected S-scan [10].	26
Figure 1.19 Dynamic depth focusing principle showing resultant beam from DDF.	26
Figure 1.20 Number of publications on PoD in the field of NDT [24].	31
Figure 1.21 Comparison of log odds and cumulative log normal models [27].	35
Figure 1.22 PoD (a) calculations from \hat{a} vs a relation [27].	36
Figure 1.23 Resolution before back wall (2 and 4 mm FBH) [33].	39
Figure 1.24 Results for the resolution before back wall FBHs. (left: conventional ultrasonic, right: phased array) [33].	40
Figure 1.25 PoD model results for UT: Different operators inspecting same specimen [20].	41
Figure 2.1 Representative micrograph of the St-37 specimen .	44
Figure 2.2 Representative micrograph of the 42CrMo4 (SAE 4140) specimen.	45
Figure 2.3 Representative micrograph of the SAE 316L specimen.	46
Figure 2.4 Schematic view of the specimen type 1.	47

Figure 2.5 Type 1 specimen preparations with CNC vertical lathe	48
Figure 2.6 The basic principle of Electrical Discharge Machining.....	49
Figure 2.7 Hole drilling with using Electrical Discharge Machining	50
Figure 2.8 Schematic view of the specimen type 2.....	50
Figure 3.1 Four possible a vs \hat{a} models for Type 1 UT specimen.....	59
Figure 3.2 Four possible a vs \hat{a} models for Type 1 Phased Array specimen	60
Figure 3.3 Four possible a vs \hat{a} models for Type 2 / St-37 UT specimen.....	60
Figure 3.4 Four possible a vs \hat{a} models for Type 2 / St-37 PA specimen.....	61
Figure 3.5 Four possible a vs \hat{a} models for Type 2 / SAE 4140 UT specimen.....	61
Figure 3.6 Four possible a vs \hat{a} models for Type 2 / SAE 4140 PA specimen.....	62
Figure 3.7 Four possible a vs \hat{a} models for Type 2 / SAE 316 UT specimen.....	62
Figure 3.8 Four possible a vs \hat{a} models for Type 2 / SAE 316 UT specimen.....	63
Figure 3.9 a vs \hat{a} parameter inputs for UT specimen (left) and Phased Array specimen (right).....	64
Figure 3.10 a vs \hat{a} linear models of UT Type 1 specimen	65
Figure 3.11 a vs \hat{a} linear models of Phased Array Type 1 specimen	65
Figure 3.12 a vs \hat{a} linear models of Type 2 / St-37 specimen (UT).....	66
Figure 3.13 a vs \hat{a} linear models of Type 2 / St-37 specimen (PA)	67
Figure 3.14 a vs \hat{a} linear models of Type 2 / SAE 4140 specimen (UT).....	67
Figure 3.15 a vs \hat{a} linear models of Type 2 / SAE 4140 specimen (PA)	68
Figure 3.16 a vs \hat{a} linear models of Type 2 / SAE 316 L specimen (UT).....	68

Figure 3.17 a vs \hat{a} linear models of Type 2 / SAE 316 L specimen (PA).....	69
Figure 3.18 PoD curve of Type 1 specimen (UT).....	70
Figure 3.19 PoD curve of Type 1 specimen (PA).....	70
Figure 3.20 PoD curve of Type 2 specimen (St-37 / UT).....	72
Figure 3.21 PoD curve of Type 2 specimen (St-37 / PA).....	72
Figure 3.22 PoD curve of Type 2 specimen (SAE 4140 / UT).....	74
Figure 3.23 PoD curve of Type 2 specimen (SAE 4140 / PA).....	74
Figure 3.24 PoD curve of Type 2 specimen (SAE 316 L / UT).....	75
Figure 3.25 PoD curve of Type 2 specimen (SAE 316 L / PA).....	75

LIST OF TABLES

TABLES

Table 1.1 Advantages and Disadvantages of Ultrasonic testing.....	4
Table 2.1 Chemical composition of St-37steel [37].....	44
Table 2.2 Chemical composition of SAE 4140 steel	45
Table 2.3 Chemical composition of SAE 316 L steel	46
Table 2.4 Data retrieved from specimen type 1 by ultrasonic method (for the flaws 2 mm in diameter located at different depths)	53
Table 2.5 Data retrieved from St-37 specimen by ultrasonic method	53
Table 2.6 Data retrieved from SAE 4140 specimen by ultrasonic method... ..	54
Table 2.7 Data retrieved from SAE 316 L specimen by ultrasonic method	54
Table 2.8 Data retrieved from specimen type 1 by phased array method (for the flaws 2 mm in diameter located at different depths).....	55
Table 2.9 Data retrieved from St-37 specimen by phased array method.....	56
Table 2.10 Data retrieved from SAE 4140 specimen by phased array method.....	56
Table 2.11 Data retrieved from SAE 316 L specimen by phased array method.....	57
Table 3.1 Reliability values for ultrasonic (UT) and phased array (PA) systems ...	76

CHAPTER 1

INTRODUCTION

1.1 GENERAL

Nondestructive testing (NDT) is an interdisciplinary and very broad field playing crucial role in order to maintain assets and systems reliable and sustainable. The most important feature of NDT implementations is that tests do not affect current and future usefulness of the material which means that NDT allows inspecting materials without damaging them.

Since its first use, many industrial related professionals are already familiar with some NDT technologies from medical to industrial usage. As the technology develops, the number of advance inspection methods grows daily, but as a quick summary of most common used methods are provided below.

- Visual testing
- Ultrasonic Testing
- Radiographic Testing
- Eddy Current Testing
- Magnetic Particle Testing
- Dye – Penetrant Testing

Based on above conventional NDT systems, some advanced NDT systems have been developing by researchers. These methods aim to improve the flexibility, reliability of the techniques and to provide easy interpretations.

Phased Array (PA) is one of the advanced NDT systems recognized in most of industrial fields. The applications of Phased Array can be seen on several industries like medical, oil & gas and aviation. This advanced system has emerged in the past few years as a very comprehensive type of conventional Ultrasonic testing.

Ultrasonic testing (UT) is maybe the most widely used method in NDT systems. The intention of using Ultrasonic system is the characterization the flaw properties with using ultrasonic waves created by transducers as mechanical vibrations. As a common practice, single element transducers are used. In this type, ultrasonic wave are generated and received on same crystal. Additionally, two paired elements are also used.

In Phased array method, it's aimed to use more than one sound wave for improving the flexibility and reliability of system with using transducer assemblies. These assemblies can consist from 16 to 256 small individual elements.

Despite the alternative conventional inspection methods, improvements of existing testing systems and intensive training strategies, inspection held by NDT systems still include some false indications, mismatched results which are simply not perfect. Therefore, since 1970s, the quantifying the reliability of NDT methodology using Probability of Detection (PoD) has been gaining crucial importance in applications.

The aim of this thesis was to implement the Probability of Detection concept in Ultrasonic and Phased Array techniques with using different types of steel specimens having well-defined artificial flaws. The result, by considering the effect of microstructure was compared.

1.2 ULTRASONIC TESTING

1.2.1 History and Introduction of Ultrasonic

The term “Ultrasonic” is the execution of ultrasound phenomena. A sound pressure oscillating by a transducer creates ultrasound which is located in a greater frequency range compared to the human hearing range. Its usage is very wide starting from sonography (ultrasound imaging) for medical purposes to Nondestructive testing of materials [1].

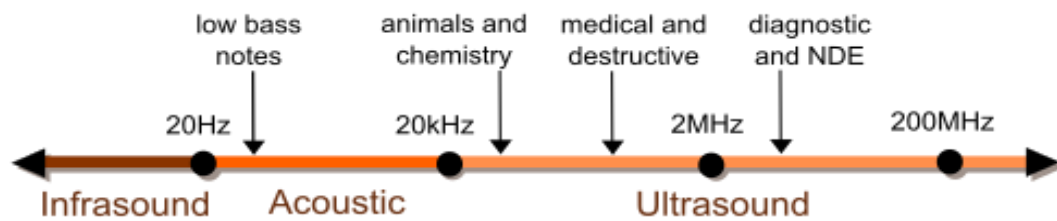


Figure 1.1 Frequency ranges of ultrasound in different applications [1].

The greatest development of ultrasonic like very similar to many engineering disciplines' industrial usages is shown in the latest 19th and 20th centuries. After ultrasonic waves' ease of producibility, it can be said that the ultrasonic were accepted as a commonly used Nondestructive method. Mulhauser in 1931 was awarded the first patent for flaw detection with using tow transducers. Following that, in 1940 Firestone and in 1945 Simons were first inventors of pulse – echo technique used in ultrasonic testing which was the fundamentals of modern testing methods today [2].

Today, ultrasonic testing has very widely applications ranging from aviation, oil & gas, railway, automotive, fabrication, power, medical industries and more. The technique's primary application is to determine and characterization of surface and subsurface flaws and discontinuities. The location and presence of imperfections like laminations, cracks, cavities and etc. are determined by defining and analyzing the reflected sound waves from interfaces.

With latest improvements of ultrasonic testing, apart from surface and subsurface discontinuities, defining bond characteristics, determination of physical properties and material structures, grain sizes and measurement of internal and external corrosion can be determined [3].

1.2.2 Advantages & Disadvantages of Ultrasonic Testing

The importance and advantage of ultrasonic testing come from its flexibility and robustness. Addition to that, the capability of determination the subsurface flaws could be counted. Only X-ray methods apart from ultrasonic testing can detect subsurface flaws. Techniques like Eddy current and Magnetic particle testing can locate some subsurface discontinuities which are very close to the surface. Moreover, ultrasonic method is eliminating the risks for health and environment with respect to Radiography. Ultrasonic testing can be used in various types of materials from biological materials to metals, ceramics to composites. However there are some disadvantages of this method. The most important disadvantage is the requirement of highly skilled and experienced technician. Also, the cost of the ultrasonic methods can be excessive. In addition, apart from non-contacting advanced methods, most of the ultrasonic systems require a coupling layer with object like through a water or gel couplant. For a general review of pros and cons of ultrasonic testing can be found on Table 1.1.

Table 1.1 Advantages and Disadvantages of Ultrasonic testing

Advantages of Ultrasonic Testing
• High penetrating capability
• High detection sensitivity and accuracy than other methods in determining size, location, characterization of interior defects
• Portability and highly automated operation capability
• Need to be accessed only one surface of component
• Non-hazardous operations

Table 1.1 (Continued)

Disadvantages of Ultrasonic Testing
<ul style="list-style-type: none">• Extensive technical knowledge, skilled and experienced operator needed.
<ul style="list-style-type: none">• Irregular shapes, very thin or small or inhomogeneous parts have inspection difficulties.
<ul style="list-style-type: none">• Surface preparation shall be made by removing paint, rust and cleaning.
<ul style="list-style-type: none">• Couplant need to be used unless a non-contact system would be used.
<ul style="list-style-type: none">• Reference standards shall be used both for calibration and characterizing

1.2.3 Theory of Ultrasonic Testing

In order to understand the philosophy behind ultrasonic, it's crucial to understand the behavior of the wave phenomena. A wave can be called as a disturbance that travels through its medium. If an atom would be forced or disturbed from its equilibrium condition, this propagates a mechanical wave without transport of matter, only transport of energy. Water waves propagating away from the source when a stone dropped can be given as example. It can be determined that across the water surface, the matter itself stills hence the water wave energy propagates.

In ultrasonic testing, mechanical vibrations based on sound waves are used. These sound waves are created by the particles oscillation in 4 different ways. These can be longitudinal, transverse (shear), surface and Rayleigh waves.

Longitudinal and transverse waves are the most used modes in ultrasonic testing. In transverse (shear) waves, the oscillation of particles is seen on the transverse to the direction of propagation. Acoustically solid material for effective propagation need to be used in order to create shear waves, therefore, in gases and liquids, these waves aren't created very effectively. On the other hand, they can easily be created in solids; hence longitudinal waves are relatively strong when compared to the transverse waves.

Longitudinal waves are also called compressional and pressure waves. They can also be created in liquids as well as solids. In longitudinal waves, the particles or atoms oscillation is seen in the direction of wave propagation, in other words, longitudinal direction.

The illustrations of longitudinal and transverse waves can be found Figure 1.2.

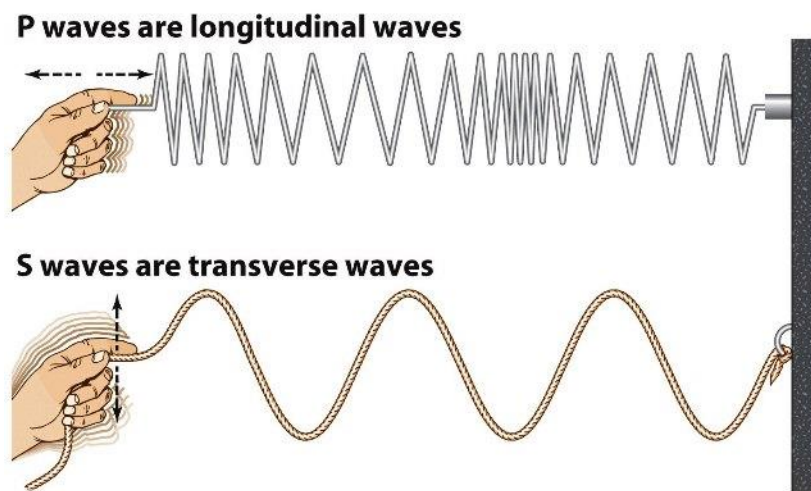


Figure 1.2 The illustrations of longitudinal and transverse waves

1.2.4 Attenuation of Sound Waves

An acoustic wave can lose its energy in some reasons while travelling through medium. It results as a decrease of its intensity with distance. In ideal condition of material, only spreading of wave caused the reducing the amplitude of sound wave. Hence in normal condition, further decrease can be seen because of scattering and absorption of sound wave called attenuation.

Absorption is the extinction the mechanical vibration in the form of heat whilst passing through the material. The result of absorption is the permanently loss of energy and not much use in ultrasonic inspection.

Another type of attenuation is the dispersion. This mechanism is occurred due to the difference velocities of sound waves in different wave modes in different materials. A study made by Ping He regarding the effect of two different types of materials to the attenuation. The experimental results of two specimens show an excellent agreement between measured dispersion and the dispersion determined from the measured attenuation with using a time causal model. The rubber material is highly attenuative and its attenuation has a non-linear frequency dependency while the Plexiglas shows a moderate attenuation that increases linearly with frequency [4]. The most important and effective factor of ultrasonic wave attenuation is scattering. The exact nature of scattering effects in solids may be referenced to different causes. Ultrasound waves' refractions, diffractions and reflections resulting from surface roughness, discontinuities in the material, and inhomogeneity in medium and grain boundaries can be counted causes of scattering and attenuation. These mechanisms can lead to considerably amount of energy losses which can render the inspection impracticable.

Above mentioned scattering mechanisms on the other hand, can be used for determination of material identification studies where grain size measurement, surface roughness and material properties (elastic moduli, Poisson's coefficient) determination needed to be done.

As an example of using scattering mechanisms for determination the material properties, a study was held by Gür et al. regarding the determination of graphite nodularity in ductile cast irons. In the experiments, cast iron specimens with different nodularity percentages were cast by the addition of different amounts of alloys to the melt and various heat treatments were applied. As a result, it was determined that the sensitivity of ultrasonic velocity and apparent attenuation against the changes in the nodular graphite content allows grading of nodular cast irons. Also it is implied that the possibility of detection of local unnodularized zones in the castings can be achieved using ultrasonic. Below figure shows the apparent attenuation amount changes with the amount of nodular graphite [5].

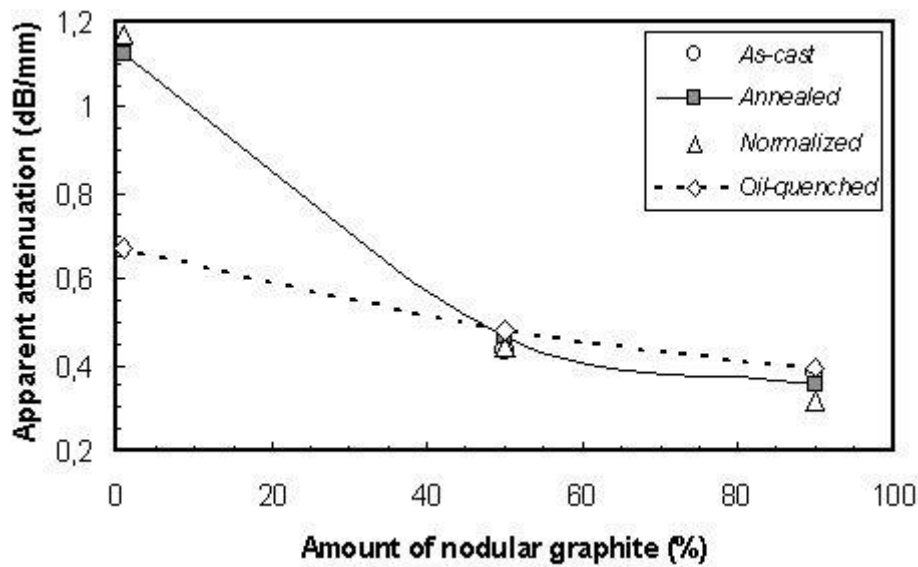


Figure 1.3 Variation of apparent attenuation with respect to amount of nodular graphite [5].

1.2.5 Ultrasonic Equipment and Transducers

Various transducers systems are using to create ultrasonic waves. The piezoelectric method is the most common method for transmitting and receiving of ultrasonic waves. But there are several other techniques are using to create ultrasonic waves like electromagnetic acoustic transducers (EMAT) and laser (optical) transducers.

1.2.5.1 Piezoelectric transducers

The first fundamental studies regarding the piezoelectric effects made in 1880s. By Jacques and Pierre curie in 1880s and “direct piezoelectric effect” was discovered. In “direct piezoelectric effect”, they stated that a piezoelectric material responds to a mechanical deformation by developing an electrical charge on its surface. This phenomenon relates the applied mechanical stress to the output charge and is a measure of the quality of the material as a receiver. Following to that, in 1881, Lipmann discovered the reverse phenomenon, “indirect piezoelectric effect” and stated that a mechanical deformation is produced when the piezoelectric material is subjected to an electric field. Thus the indirect piezoelectric effect relates the input

charge on the material surface to the output strain, and is a measure of the quality of the material to generate sound [2].

As described above, in transmit mode, ultrasonic is created by piezoelectric transducers by converting electrical signals into mechanical vibrations and vice versa in receive mode. They can be naturally occurred or artificially produced. Quartz may be the best naturally occurring piezoelectric material known. Barium titanate (BaTi), lead metaniobate (PMN) and lead zirconate titanate (PZT) are also known as the most used artificial piezoelectric materials. Additionally, composite transducers, in recent years, are gaining importance in the production of piezoelectric materials.

1.2.5.2 The characteristics of Piezoelectric Transducers

Piezoelectric transducers can be categorized by the generated wave type, beam orientation, usage environment, etc... Some of the most common categorization of the piezoelectric transducers is;

- Wave type (longitudinal or transverse)
- Beam type (normal beam or angle beam)
- Element number (single element or multiple element)
- Transducer face type (flat face or shaped face)
- Contact type (immersion, water coupled or air coupled)

Transducers can be categorized with their type of generated waves. As an example, the quartz crystal transducers' wave type can be determined as longitudinal or transverse by the way of cut.

Piezoelectric transducers also categorized as angled or normal beam. Transmitted wave travels normal to the face of transducer in normal beam transducers, on the other hand, in angle beam transducers; wave is transmitted at an angle to the face of transducer. Angle beam transducers are generally transformed into normal beam

transducers with using wedges attached on their crystal. In addition to angle beams, with using wedges, longitudinal, shear and surface waves can be created as well.

Piezoelectric transducers generally contain multiple elements. Dual element transducers allow improvement of resolution of near surface by containing a transmitter and a receiver housed in its case. In another application is using more than 2 piezoelectric transducers. They act together and create an array. If each transducer wave transmitted in slightly different times interferes constructively in a selected angle, then the system is called phased array.

In most applications, flat or normal face transducers are used. But shaped face transducers are also common. Their advantage is coming from matching the sample contour and focusing the ultrasonic wave.

Transducers also categorized as contact, immersion and air – coupled as per coupling types. Contact types are directly contacted with specimen surface but need some form of couplant to transmit the wave to the test sample and vice versa. Due to the impedance difference of air and transducer, special layer of material is needed to be used in this type. This impedance matching layer helps to send a pulse through air to specimen.

Immersion configuration of ultrasonic testing operates in a scanning atmosphere where the transducer and sample are contacted with immersion fluid, typically water.

1.2.5.3 The characteristics of Piezoelectric Transducers Beams

The ultrasound created by piezoelectric transducer originated from the surface of the piezoelectric crystal instead a single point of crystal. Since the originated waves coming from several different units along the crystal surface, the intensity of ultrasound beam might be affected by destructive and constructive interferences. These interferences in the sound intensity can be lead to strong fluctuations near the source which is known as near field.

In near field or Fresnel zone, along the central axis of the sound beam, the acoustic sound wave pressure variations are broader and widely spaced linearly as crystal face increases. Due to this mechanism, it can be very difficult to evaluate the flaws accurately when their location is in this section of specimen. Where the crystal face becomes to near field length, the acoustic pressure reaches a maximum magnitude and decreases exponentially with increasing distances as shown in Figure 1.4.

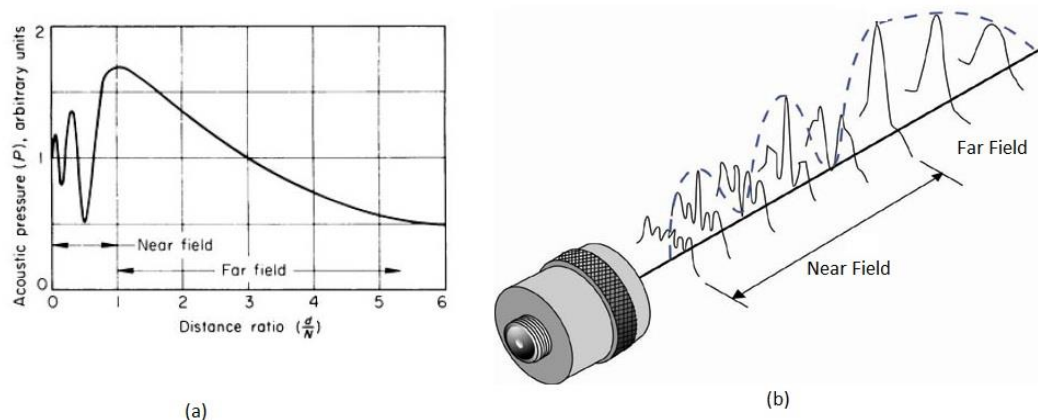


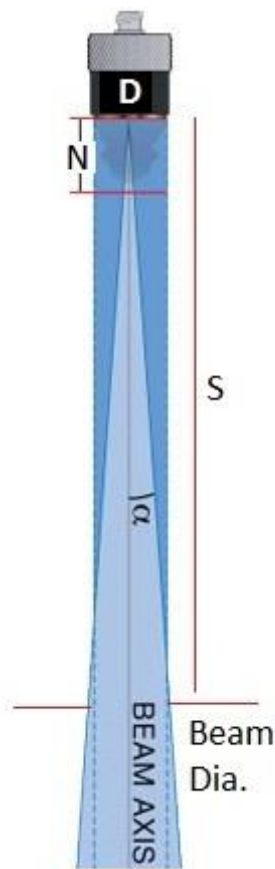
Figure 1.4 (a) Variations of acoustic sound pressure with distance ratio for circular crystal. (b) Schematic sound field.

The length of near field is determined by the size of piezoelectric crystal and wave length.

$$N = \frac{D^2}{4 \times \lambda} \quad (\text{Eq. 1.2.5.3}) \quad \text{or} \quad N = \frac{D^2 \times f}{4 \times c} \quad (\text{Eq. 1.2.5.3a})$$

Where N is near field distance (mm), f is frequency (Hz), λ is wavelength (mm), c is sound velocity in the material (m/s), and D is the crystal diameter (mm).

Distances greater than near field (N) are known as the far field of ultrasonic beam. This area is also known as Fraunhofer zone where the maximum sound pressure always can be found along the centerline of the transducer crystal. Due to above reasons the strongest reflections can be retrieved from as mentioned area of ultrasonic beam.



$$D_{efficient} = 0,95 \times D \quad (\text{Eq. 1.2.5.3 - 2})$$

$$(D_B)_{-6dB} = \frac{\lambda \times s}{D} \quad (\text{Eq. 1.2.5.3 - 3})$$

$$(D_B)_{-20dB} = \frac{2 \times \lambda \times s}{D} \quad (\text{Eq. 1.2.5.3 - 4})$$

$$(\sin \alpha)_{-6dB} = \frac{\lambda}{2 \times D} \quad (\text{Eq. 1.2.5.3 - 5})$$

Where s is sound path, v is angle of divergence.

Figure 1.5 Schematic views of ultrasonic beam spread and divergence

1.2.5.4 Other Ultrasonic Equipments

Most of the ultrasonic inspection systems include following equipment;

- A variable to be measured
- Producing burst of alternating voltage by electronic signal generator
- Transducer emitting ultrasonic wave beams (longitudinal, shear, surface, etc...)
- Couplant that transfer ultrasonic beams to the specimen
- Transducer accepts and convert ultrasonic waves to burst of alternating voltage coming from test specimen
- A display device, usually a cathode ray tube (CRT), to characterize and record the output.

With above system, ultrasonic testing can be used for corrosion mapping, thickness gauging and flaw detection in various types of metals, composites, polymers and ceramics.

1.2.6 Ultrasonic Measurement Systems

There are two major ultrasonic inspection methods are existed, pulse – echo and transmission methods. Also the applications of ultrasonic are used in other techniques like spectral analysis, acoustical holography and acoustical microscopy.

1.2.6.1 The Transmission Method

In transmission method, the only concern is to measure the signal attenuation, hence in pulse – echo method, both the signal attenuation and the transmit time are measured.

The transmission method may include reflection and through transmission. The main concern in this method is to determine any signal attenuation. But this method also used in flaw detection as well. Flaws, in this method, are determined by comparing the intensity of ultrasound wave transmitted through specimen with the intensity transmitted through a reference block.

The test method requires two units, one for transmit and one for to receive the ultrasound waves. Immersion techniques, water column techniques are most used ones due to their effective and uniform coupling properties between the transducers and specimen.

Through transmission ultrasonic technique are broadly implemented in many industrial applications due to their ability to perform characterization and long term monitoring of material properties. This technique is sufficiently fast to enable monitoring deviations of thickness or ultrasound velocity under industrial conditions.

Raisutis et al uses cross – correlation function between the transmitted through immersed test sample and the signal transmitted through water between transducers. And they measured the time interval between these two signals to determine the estimation of phase velocity dispersion in highly attenuating planar PVDF sample [6].

1.2.6.2 The Pulse – Echo System

The pulse – echo method is the most widely used ultrasonic inspection method, incorporates with a single transducer both transmitting and receiving the ultrasonic wave. The pulse – echo system has several advantages due to the dual function of the probe, which is simplifying the system. Additional to that, the system gives advantage where the specimen accessibility is limited. Only one side access is enough to complete the inspection.

On the other hand, pulse – echo system has some disadvantages as well. One of the disadvantages of pulse – echo system is the main bang. The main bang is generated when the receiver sees the electric pulse generated by transducer. This pulse's intensity is large which a necessity is. As a result, very sensitive receiver electronics are saturated. The main bang appears in the system as a large and off – scale initial echo. This first echo, additionally, can create a dead zone in the received signal, which can cause a signal detection difficulty if the defect or discontinuity is near to the surface. Moreover, due to the overlapped multiple returning echoes make signal detection difficulties in pulse – echo system with a near surface flaw or for thin materials.

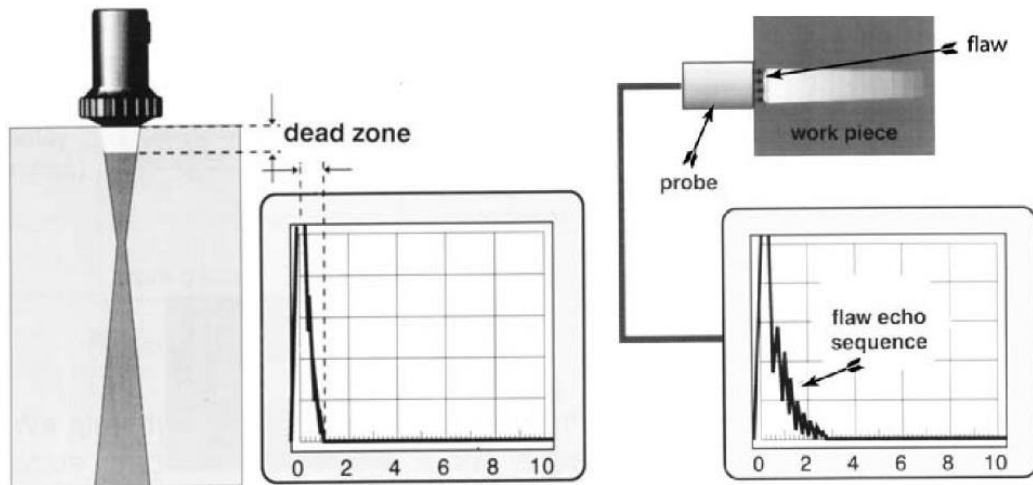


Figure 1.6 Dead zone in pulse – echo system (left) and overlapping echoes from multiple reflections.

1.2.7 Data Presentation of Ultrasonic Testing

Both conventional and advanced ultrasonic systems utilize high frequency sound waves to check internal structure of material and measure thicknesses. All data utilized by systems are gathered and displayed in different formats for interpretation and evaluation easiness. These presentation modes provide different images of material being inspected.

Most common formats are known in ultrasonic systems are A – Scan, B – Scan, C – Scan and S – Scan presentations. Advanced ultrasonic systems have the capability to display all data in all presentation modes simultaneously.

1.2.7.1 A – Scan Presentation

A – Scan presentation is the most basic mode in ultrasonic systems. In this method, the echo amplitude and transit time of ultrasonic waves are plotted on a grid with vertical and horizontal axis. Usually, vertical axis shows amplitude and horizontal axis represent time or distance.

In A – Scan presentation, discontinuity property (size) can be relative measured with comparing the signal amplitude retrieved from a known reflector.

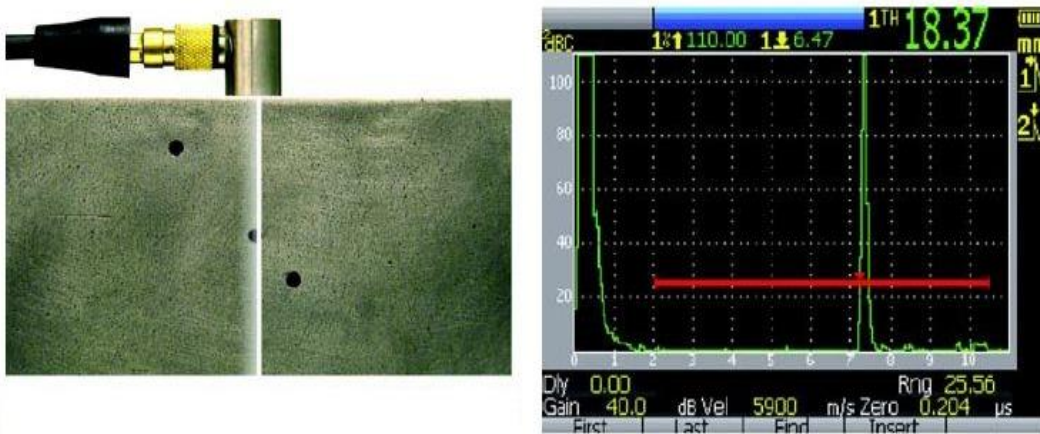


Figure 1.7 Typical A-Scan presentation [7].

1.2.7.2 B – Scan Presentation

B – Scan imaging gives the profile / cross – sectional view of the test specimen. In B – Scan presentations, the thickness is plotted as a function of time or distance same with A – Scan, but additionally, the depth profile of scanned part can also be provided. In B – Scan imaging, the user can easily visualize both near and far surface reflectors within the sample. An example below shows the details of B – scan imaging system.

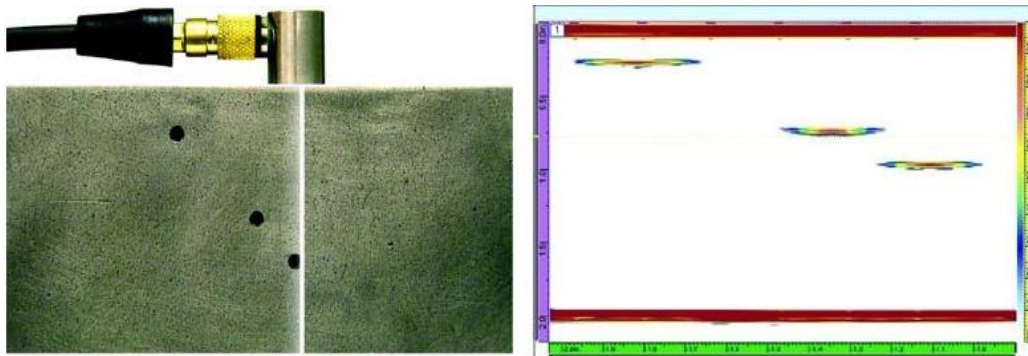


Figure 1.8 Typical B – Scan presentation [7].

1.2.7.3 C – Scan Presentation

C – Scan presentation is a two dimensional imaging system showing the top or planer view of specimen. It is similar in graphical point of view with x-ray imaging. In C – Scan imaging, color represents the depth at each point and location of the reflector in the test piece.

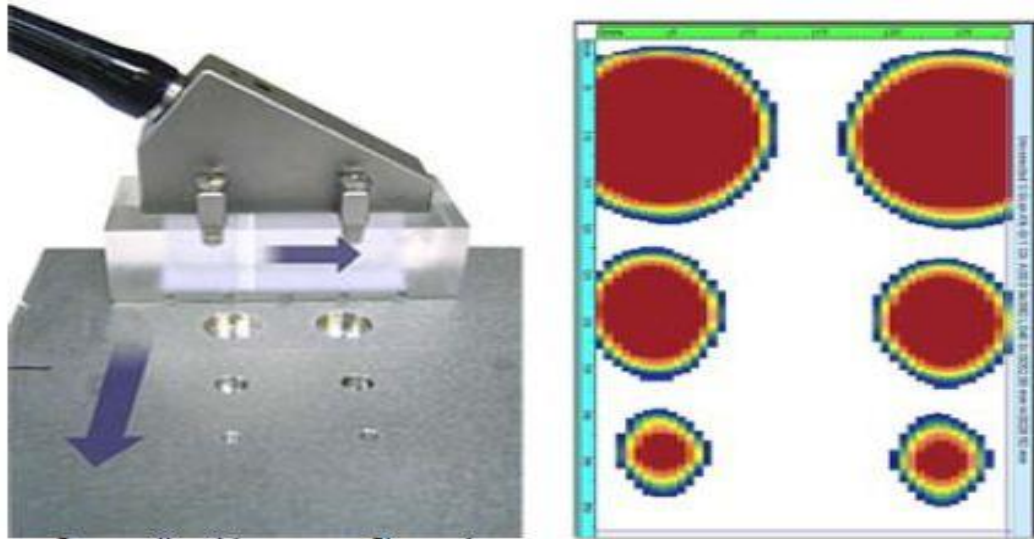


Figure 1.9 Direction of motion and C-scan image showing the reflectors (holes) position [7].

1.2.7.4 S – Scan Presentation

S – Scan imaging is unique to the phased array equipment. Fixed apertures and steering through a sequence of angle properties of phased array equipment are used in this presentation type.

Two main forms are typically used. The most familiar and common type uses a zero degree interface wedge to steer longitudinal waves creating a pie type image. The other type on the other hand uses a plastic wedge to produce the transverse waves in the refracted angle range of 30 to 70 degrees. The technique is very similar to conventional beam angle inspection hence, the beam sweeps through a range of angles rather than a fixed, single angle.

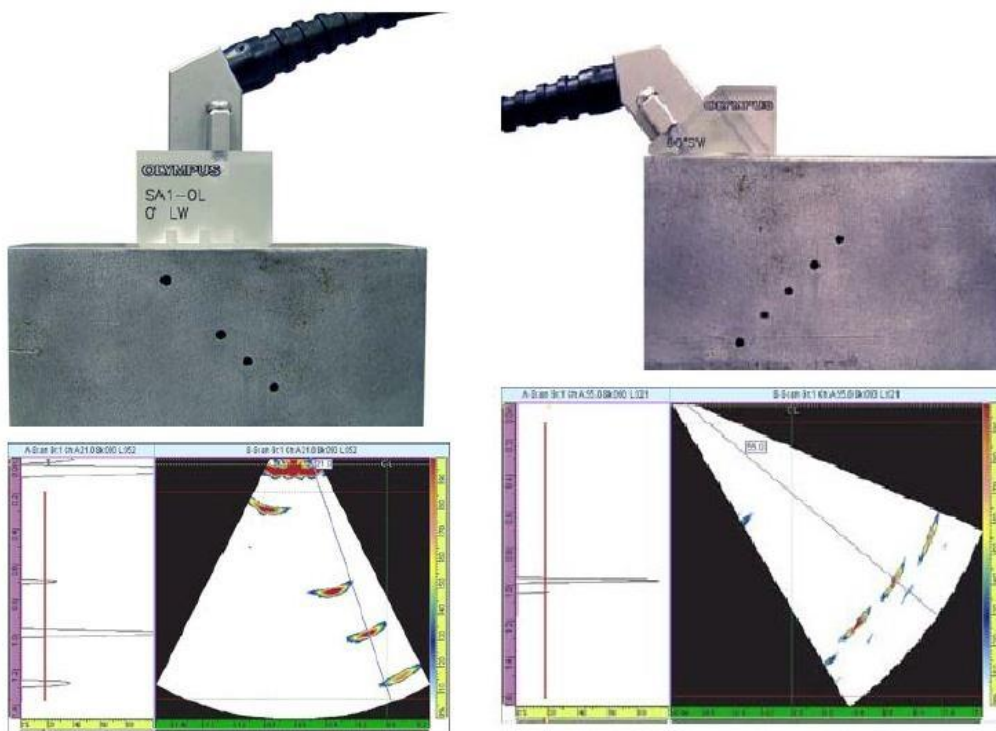


Figure 1.10 Zero degree wedge, longitudinal waves $-30 - +30^\circ$ S-scan image (left), Shear waves in the refracted angle between $+35 - +70^\circ$ S-scan image (right) [7].

1.3 PHASED ARRAY SYSTEM

1.3.1 General Introduction and History of Phased Array System

Ultrasonic phased array system has become a very powerful form of applied ultrasonic testing in NDT applications in recent years. This technology has been, around for 60 years, started with medical industry usages. The medical industry has been pioneering many of industrial imaging systems and phased array also one of them. Due to the computerized systems' lack of usage and also the cost reasons, unfortunately, NDT industry has been relatively slow to catch up the new technology [8].

First usages of ultrasonic phased array systems were started around end of 1960s. The system applications were confined to predict the composition, structure of human body and make medical diagnosis. Industrial applications on the other hand,

were started lately, in 1980s, due to the widely varying acoustic properties of specimens (metals, ceramics, composites and etc...) and also the varying thicknesses and geometrical properties. The first application examples of phased array systems were used in-service power generation inspections which require huge data amount and data transfer ability for processing and image presentation. Also largely manufactured shafts, turbine component and especially nuclear power generation equipment were examples of first industrial phased array systems due to its greater Probability of Detection [7].

In 2000s, battery powered and portable phased array equipment appeared for industrial usage. The technological rapid development in microelectronics, the availability of better power saving batteries enabled more rapid development of phased array equipment's next generation. As a result, new phased array tools are portable including electronic setup, data processor, analyzer and display, even with a touch screen.

1.3.2 Basic Principles of Phased Array

Conventional ultrasonic transducers consist of either a single element both generate and receive sound waves or two paired elements for transmitting and receiving separately. Besides, Phased array ultrasonic is a process wherein multi-element transducers are used and constructive phase interference by accurate time delayed pulses are created by these transducers [9]. These multi element probes typically can be pulsed separately. These pulsing can be arranged in different type of probe shapes like linear array probe, annular array probe, more complex shaped probes and etc... Additionally, phased array probes can be designed for direct contact usage or can be assembled with a wedge as well.

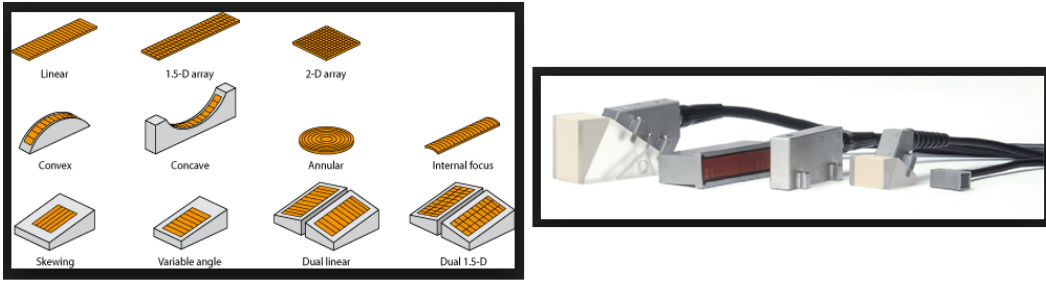


Figure 1.11 Different shaped and wedged phased array probes

Ultrasonic waves are mechanical vibrations induced in an elastic medium by the piezocrystal probe excited by an electrical voltage. Single crystal probes using divergent beams are generally used in conventional ultrasonic inspections. Hence, in order to increase the resolution of flaw and decrease the dead zone, dual element probes or monocrystals with focused lenses are used in some cases. But in all cases, the ultrasound wave propagates as a single refracted angle along an acoustic axis. This leads the sizing and detection limitation due to the single-angle scanning pattern. In order to eliminate the disadvantage of conventional system, multielement phased array probe using focused beams activated by hardware and analyzed by software was created.

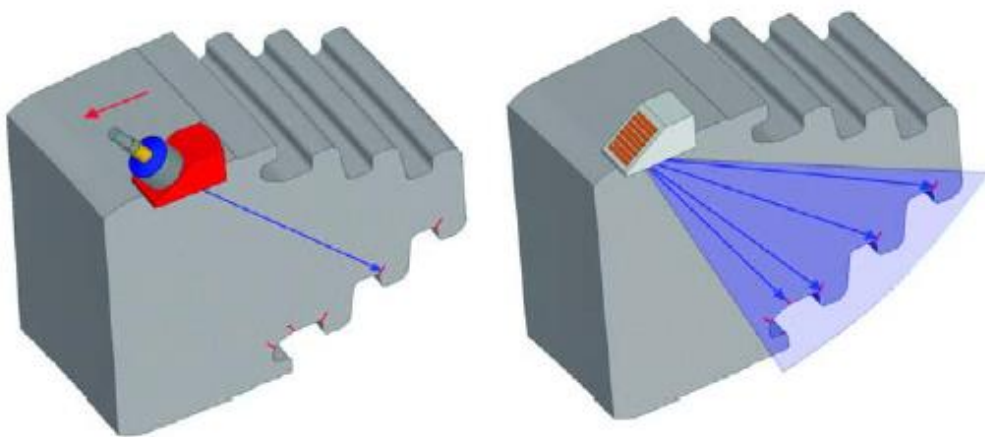


Figure 1.12 Multiangle scans and probe movement requirement on monocrystal inspection (left), Focused beam through required region without probe movement on linear array probe (right) [10].

Above mentioned multiple element probe are used whereby the output pulse from each element is time delayed in such a way so as produce constructive interference at a specific angle and a specific depth. These time delays can be incremented over a range of angles to sweep the beam over the desired angular range. For instance, 40 to 75 degree beam sweep would be produced by calculating the time delays to produce constructive interference at 40, 41, 42 ...75 degrees. This NDT technology is also referred as Swept Beam Ultrasonic testing.

The main advantages of phased array in NDE are:

- Ability to sweep a range of angles
- Ability to display the image in real time to produce swept angles
- Ability to focus [11]

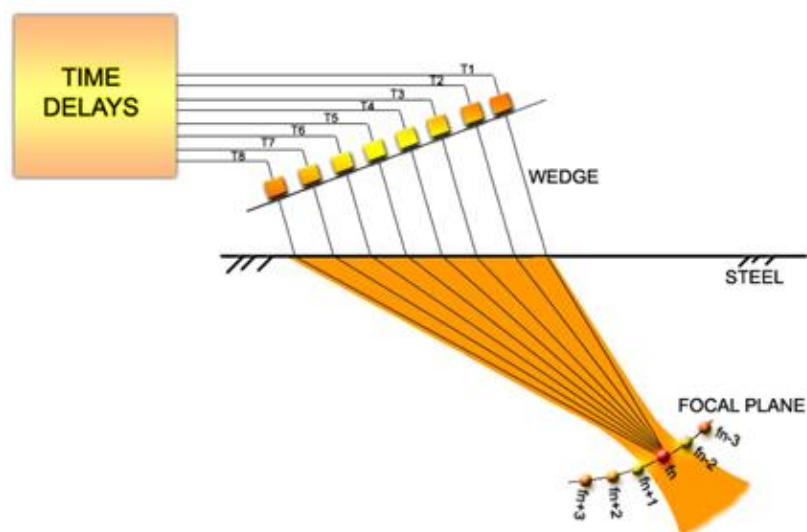


Figure 1.13 Focusing control and beam sweeping using time delays of multiple elements [11].

A phased array system utilizes the wave propagating with the principle of phasing. Phase shifting/phasing is a controlling process to bend, steer or focus the energy of a wavefronts by controlling the interactions using time-shifting wavefronts that originate from two or more sources.

The system varies the time between series of ultrasonic pulses in such a way that the individual wavefronts generated by each element in the array combine with each other. This action adds or cancels energy in predictable ways that effectively steer and shape the sound beam. This accomplished by pulse the individual probe elements at slightly different times.

The programmed pulsing sequence selected by the instrument's operating software then launches a number of individual wavefronts in the test material. These wavefronts in turn combine constructively and destructively into a single primary wavefronts that travels through the test material and reflect off cracks, discontinuities, back walls and other material boundaries like a conventional ultrasonic wave. Apart from conventional ultrasonic, the beam in phased array can be dynamically steered through various angles, focal distances and focal spot sizes in such a way that a single probe assembly is capable of examining the test material across a range of different perspectives [7]. A single crystal probe with limited movement and beam angle has a high probability of missing misoriented cracks or cracks located away from the beam axis, but with the help of the possibility of modifying beam parameters such as angle, focal distance and focal spot size through software, the sweeping beam can detect in specular mode the misoriented defects.

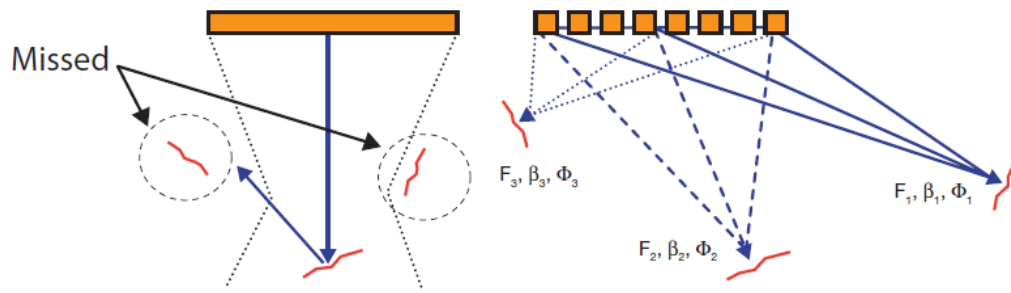


Figure 1.14 Detection of misoriented cracks by monocrystal (left) and multielement probes (right) [12].

In phased array system, while the creation of beam, ultrasonic wavefronts which time-delayed and synchronized in phased and amplitude should be rendered. Steering capable ultrasonic beam is produced by this wavefronts using the constructive interference. Additionally, for generation a phased beam with a constructive interference, the same global time-of-flight arrival of the multiple wavefronts should be assigned at the interference point. Pulsing of various probe elements at coordinated and slightly different times can lead to achieving of this effect.

Below figure shows the echo from the desired focal point hits the various transducer elements with a computable time shift. The echo signals received at each transducer element are time-shifted before being summed together. The resulting sum is an A-scan that emphasizes the response from the desired focal point and attenuates various other echoes from other points in the material.

During transmission, the acquisition instrument sends a trigger signal to the phased array instrument. The latter converts the signal into a high voltage pulse with a preprogrammed width and time delay defined in the focal laws. Each element receives one pulse only. This creates a beam with a specific angel and focused at a specific depth. The beam hits the defect and bounces back.

The signals are received, then time-shifted according to the receiving focal law. They are reunited together to form a single ultrasonic pulse that is sent to the acquisition instrument.

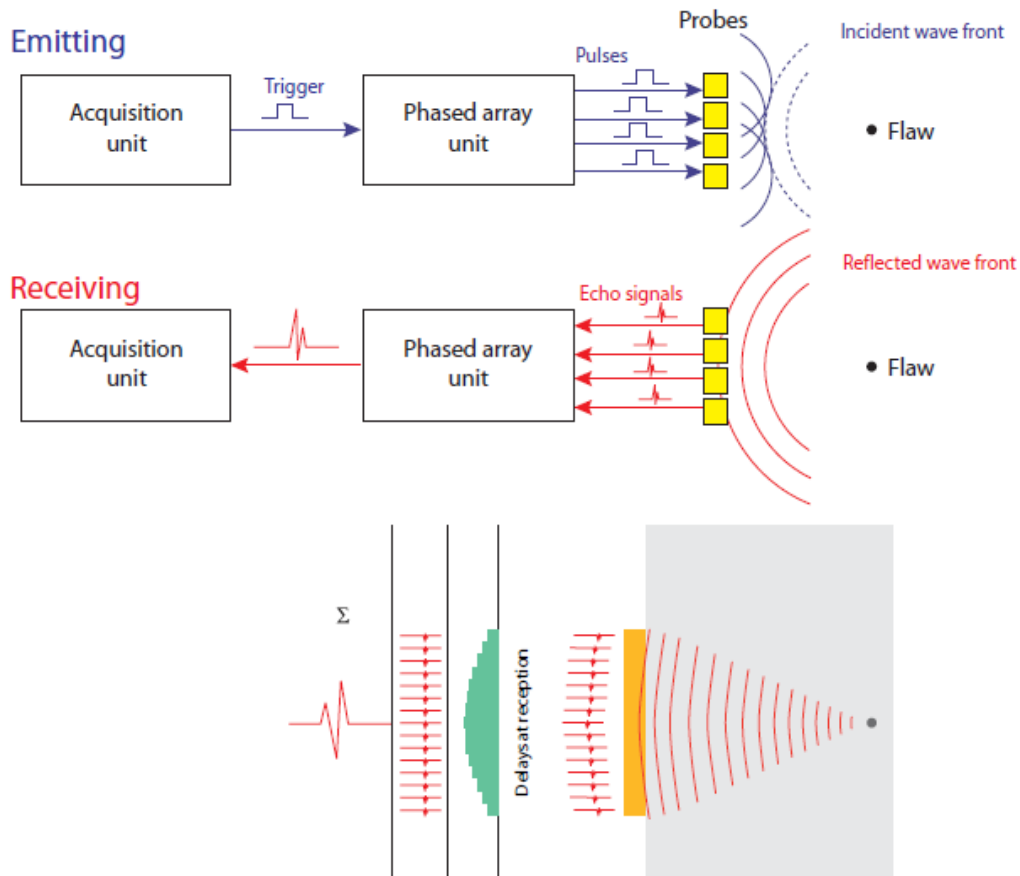


Figure 1.15 Beam forming and time delay for pulsing and receiving multiple beams [12].

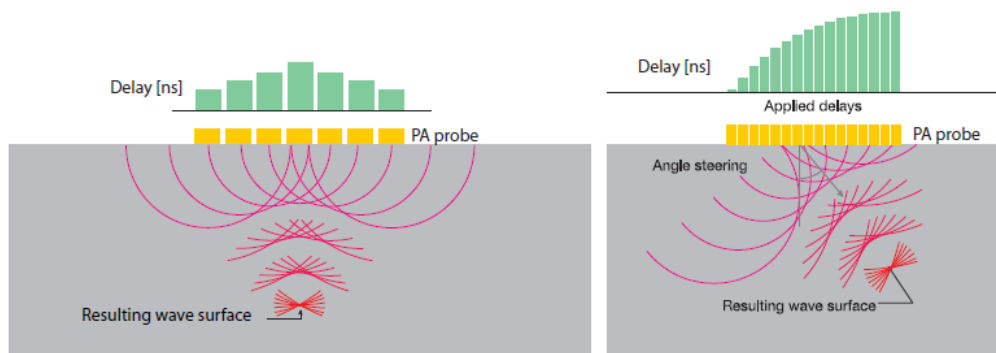


Figure 1.16 Beam focusing principle for normal (a), and angled (b) incidences [10].

There are three major computer controlled beam scanning patterns

- Electronic scanning (E-scans, linear scanning): The same focal law and delay is multiplexed across a group of active elements. Scanning performed at a constant angle and along the phased array probe length by a group of active elements called a virtual probe aperture. The equivalent to a conventional ultrasonic transducer performing a raster scans for corrosion mapping or shear wave inspection of a weld [10].

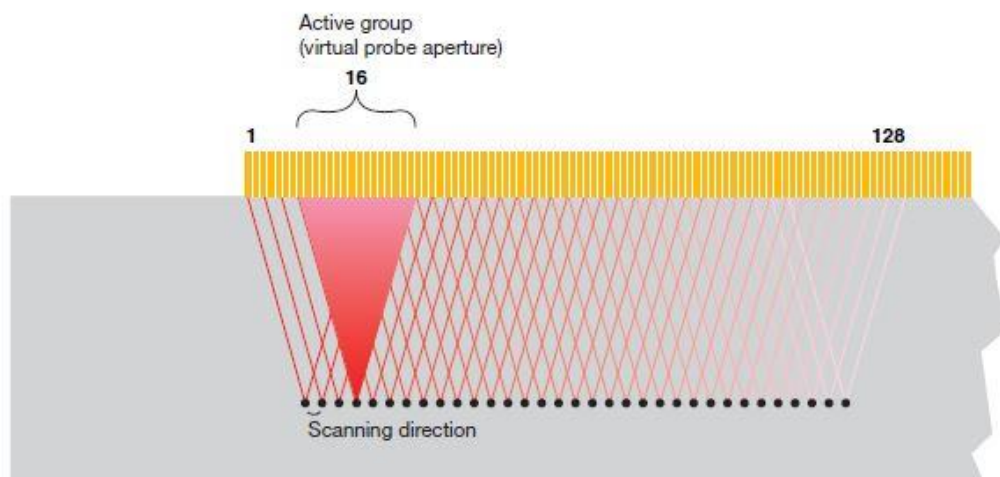


Figure 1.17 Electronic scanning with normal beam (virtual probe aperture=16 elements) [12].

- Sectorial scanning (S-scans, azimuthal / angular scanning): the beam is swept through an angular range for a specific focal depth, using the same elements. Other sweep ranges with different focal depths may be added; angular sectors could have different sweep values.

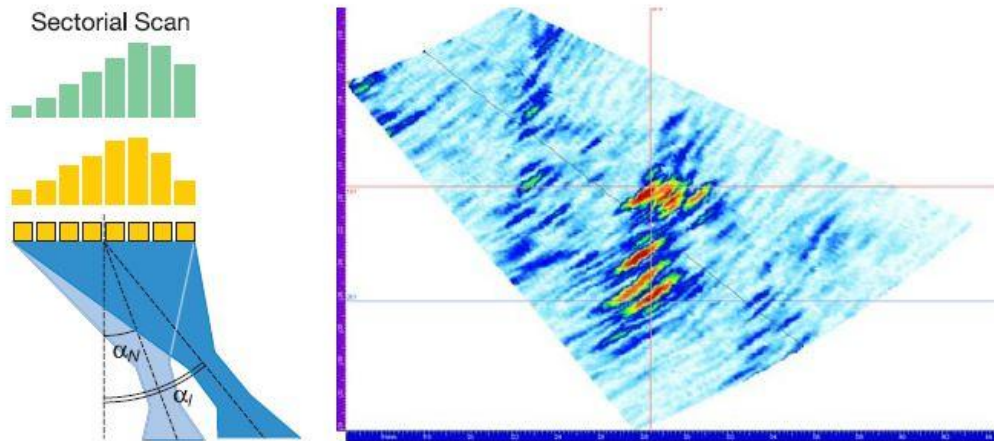


Figure 1.18 Detection a group of cracks in volume corrected S-scan [10].

- Dynamic depth focusing (DDF): DDF is a programmable, real-time array response on reception by modifying the delay line, gain and excitation of each element as a function of time. In DDF, different focal depths are used for inspection. Practically, refocusing for all programmed depths is performed after focusing using single transmitted pulse.

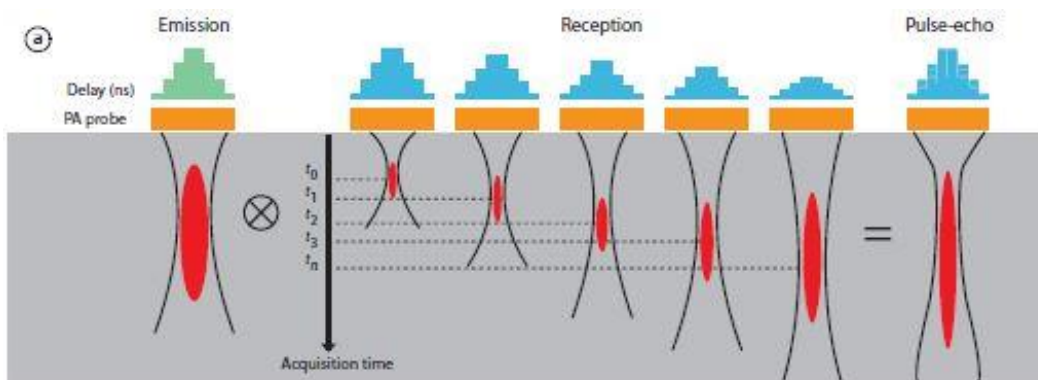


Figure 1.19 Dynamic depth focusing principle showing resultant beam from DDF

1.3.3 Advantages of Phased Array against Conventional UT

Phased array inspections can be adapted in almost any implementations where conventional ultrasonic methods have been used. In recent years, phased array techniques are finding increasing number of applications for the inspection of industrial components. Briefly, weld inspections, crack detections are the most important applications are done in a wide range of industries including petrochemical, aerospace, power generation, general manufacturing and etc...

With considering with the capability and ability of conventional ultrasonic testing, the advantages of phased array system are the following;

- Usage of multiple elements to steer, focus and scan beams with a single probe assembly.
- With the application of steering, inspection became a much more rapid process and additionally, complex geometrical specimen inspection can greatly be simplified.
- Small footprint and beam sweeping ability without moving the probe aid the inspection of specimen which has limited access.
- With using beam steering (sectorial scanning), welds can be inspected with high Probability of Detection with a single probe using multiple angles.
- Flaws determined can be located directly and evaluated immediately.
- Ultrasonic images are easy to interpret; therefore minimal operator training is required.
- The ability of focusing to the multiple depths can improve the ability of sizing defects. Study made by Jobst et al [13] shows the total focusing method superiorities against sector scan in terms of array performance and less interferences.
- The phased array inspection speeds can be as much as 10 times faster when compared with conventional UT. The ability of simultaneously test across multiple angles and/or to scan a larger area of the test pieces through linear scanning increases the inspection speed [7].

In literature, there are some researches made to assess the superiorities of inspection systems. A project [14] with nine several authorized inspection parties representing nuclear utilities, oil – gas sector, military and regulatory authorities was conducted to quantify the reliability for defect detection and sizing of manually applied phased array systems for ferritic welds. 400 flaws varying from 6 mm to 50 mm in thickness represents lack of fusion defects, cracks and volumetric discontinuities. As a result, it was statistically determined that, these operators' results the overall flaw detection rate was 96.6 % for phased array and 93.8 % for conventional UT.

Another study made by Ciorau [15] regarding the ligament evaluation on eight blocks with five EDM notches cut along each block width which are oriented are different angles from 0° from 40°. The results show that conventional ultrasonic probes cannot size the inner ligament for height < 3 mm. Moreover, accuracy in sizing is about ± 1.5 mm. Besides, phased array techniques could reliably size the ligament starting with 1.5 mm. Also it has greater accuracy with a ± 0.4 mm with compared to conventional ultrasonic.

Apart from phased array's advantages, the potential disadvantages of system are higher cost and a requirement for experienced operator need.

1.3.4 Applications of Phased Array System

In the manufacturing industry, as the manufacturing rate increases, new, innovative, fast and most importantly reliable test systems requirement gain importance. Phased array technology is leading amongst these test systems in terms of speed, reliability and data storage. Thus, in several different industries, the applications of phased array can be found;

- SCC detection and sizing in turbine roots
- Landing gear inspections
- Austenitic pipe weld inspections
- Detection and sizing of SCC in in-service piping

- Butt weld inspections
- Bolts and T-weld inspections of bridge structures
- HIC – hydrogen induces cracking
- Flange corrosion, nozzle and thread inspections
- Spindle / shaft inspections
- Composites [16]

The above application areas show that portable phased arrays can perform many different types of inspections varying from basic weld inspections to specialized inspection types. The scanning speed of phased array with a better coverage and focusing, the flexibility of system, imaging capability (S-Scan, C-Scan, etc..), different inspection angles and small footprint makes phased array as an accepted NDE technology, but the procedures and processes need to be demonstrated [17].

1.4 Probability of Detection (PoD)

1.4.1 Introduction and History of Probability of Detection (PoD)

Manufacturers are today experiencing an exceptional situation with higher demands on performance (lighter, more reliable and lower costs) and aggressive competition from all regions in the world. To be competitive on the global market, established manufacturers need to cut costs, reduce lead time to market and improve quality, simultaneously. Many industries still rely heavily on destructive testing techniques for identification of deviations such as defects and imperfections when producing components conforming to the quality requirements. Within the nuclear and aeronautic industry advanced forms of NDT have been applied both for manufacturing control (e.g. welding) and in-service inspections since more than three decades. This development was driven by the introduction of structural design and risk based inspection programs developed from the damage tolerance concept. New and stronger demands on reliability of used non-destructive methods and procedures (NDT/NDE) have enforced different strategies to quantify the inspection

capability. The most dominant and frequently used method within the aero industry is the Probability of Detection (POD) methodology [18].

PoD functions, for describing the reliability of an NDT method or technique have been the subject of many studies and have undergone considerable development since the late 1960's and early 1970's, where the most of the pioneering work was carried out in the aerospace industry. In order to ensure the structural integrity of critical components it was becoming more evident that instead of asking question "... what is the smallest flaw that can be detected by an NDT method?" it was more appropriate, from fracture mechanics point of view, to ask "... what is the largest flaw that can be missed?" To elaborate this, some real ultrasonic inspection data has been considered from the "Non-Destructive Testing Information Analysis Centre" (NTIAC) capabilities data book [19].

In 1969, a program was initiated by the National Aeronautics and Space Administration (NASA) to determine the largest flaw that could be missed for the variations NDT methods that were to be used in the design and production of the space shuttle. The methodology by NASA was soon adopted by the US Air Force as well as the US commercial aircraft industry. In the last two decades many more industries have adopted similar NDT reliability methods based on PoD [20].

PoD studies have been subjected in many more industrial areas extant nowadays. In aircraft structures, Childs et al studied X-rays radiography to detect the ceramic inclusions in Titanium castings in 1999 [21]. In nuclear energy sector, Müller et al studied PoD evaluation of NDE techniques for copper canisters for risk assessment of nuclear waste capsulation [22]. Another study was made in offshore section of oil & gas industry in early 1990's in the UK to determine the detection of fatigue cracks in tubular joints [23].

As known, the determination of Probability of Detection (PoD) is one possibility to quantify the probability to detect a specific flaw with an NDT method. Publications dealing with PoD applications can be found in different fields like medical sciences,

biology, materials science, physics, engineering sciences, telecommunication and etc.

In the field of NDT, the number of publications dealing with the topic PoD has increased significantly during last few years. This fact indicates that Probability of Detection concepts are of increasing importance when NDT methods are applied [24].

Addition to that, the American Society for Testing and Materials (ASTM), has issued a standard practice for “Probability of Detection Analysis for Hit/Miss Data”, ASTM E2862-12 [25] which also emphasizes the importance of PoD approach in NDT field.

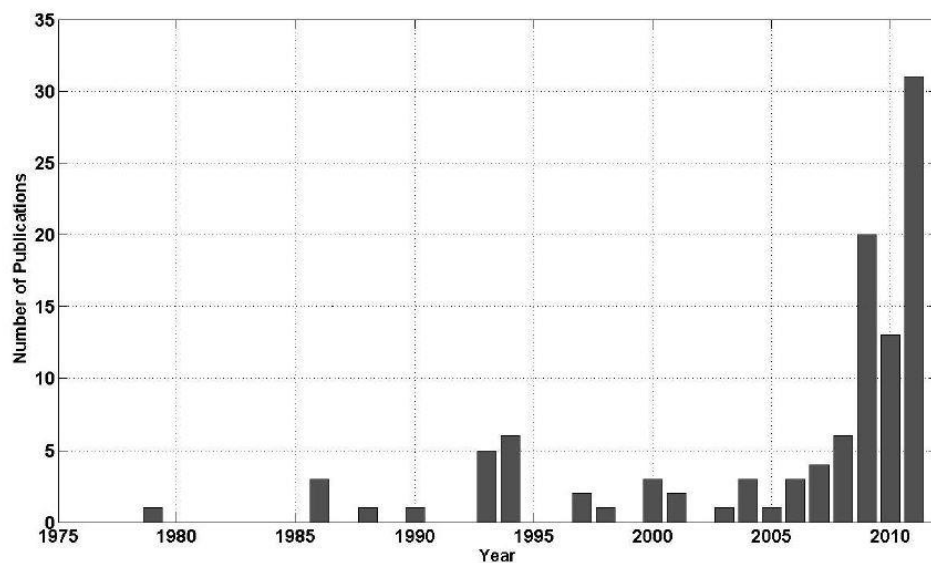


Figure 1.20 Number of publications on PoD in the field of NDT [24]

1.4.2 Usage of Probability of Detection Data

Quantifying the reliability and capability of an NDT procedure has been gaining importance in engineering applications. NDT capability levels are being combined with the life cycle management based on design parameters, the service life extensions of critical structures and basically more efficient designs.

Probability of Detection curves named very useful in providing valuable data that are obtainable from the NDT procedures in terms of reliability of the testing system. On the other hand, the validation of the reliability of each NDT procedure shall be implemented. Additionally, PoD curves also provide a viable method of quantifying the performance capability of both NDT procedure and also operator. In the light of the foregoing, PoD curves may be used as a basis for below items;

- Establishment of the design requirements
- Determination the inspection maintenance intervals
- NDT procedure and NDT personnel qualification
- Comparison of NDT procedure capabilities
- True selection of an NDT system [26]

There are two related approaches to a probabilistic framework for analyzing inspection reliability data. Originally, inspection results were recorded only in terms of whether or not a flaw was found. Data of this nature are called hit / miss data, and an analysis method for this data type evolved from the original binominal characterization. It was later observed that there is more information in the NDT signal response from which the hit / miss decision is made. Because the NDT signal response can be considered to be the perceived flaw size, data of this nature are called \hat{a} data. A second analysis method was developed based on \hat{a} data which is called signal response data [27].

1.4.3 PoD (\hat{a}) Curves from Hit / Miss Data

The name “hit / miss PoD” comes from some NDE procedures that return binary decision results of flaw detection or not. The operator or inspector exploit his/her knowledge and experience to make a decision for existence of flaw or not using specimens with different flaw properties such as size and geometry. The decision that there is a flaw is called a “hit” represented by numerical value 1; otherwise there is a “miss” represented by numerical value zero [28].

In hit / miss data analysis, the POD(a) function is defined as the proportion of all cracks of size a that will be detected in a particular application of an NDE system. Assume that each crack of size a in the potential population of cracks has its own distinct crack detection probability, p , and that the probability density function of the detection probabilities is given by $f_a(p)$. The conditional probability of a randomly selected crack from the population having detection probability of p and being detected at the inspection is given by $p f_a(p) dp$. The unconditional probability of a randomly selected crack from the population being detected is the sum of the conditional probabilities over the range of p , that is:

$$PoD (a) = \int_0^1 p \times f_a(p) \times d_p \quad (1.1)$$

Therefore, POD(a) is the average of the detection probabilities for cracks of size a . Equation (1.1) implies that the POD(a) function is the curve through the averages of the individual density functions of the detection probabilities. This curve is the regression equation and provides the basis for testing assumptions about the applicability of various POD(a) models. In studies of Berens et al [29], seven different functional forms were tested for applicability to available PoD data, and it was concluded that the log-logistics (log odds) function best modeled the data and provided an acceptable model for the data sets of the study.

Two mathematically equivalent forms of the log odds model have subsequently been used. The earliest form is given by:

$$PoD (a) = \frac{\exp(\alpha + \beta \ln a)}{1 + \exp(\alpha + \beta \ln a)} \quad (1.2)$$

This parametrization can also be expressed as:

$$\ln \left[\frac{PoD(a)}{1 - PoD(a)} \right] = \alpha + \beta \ln(a) \quad (1.3)$$

In the Eq. (1.3), the log of the odds of the PoD is expressed as a linear function of $\ln(a)$ and is the source of the name of the log odds model. Maximum likelihood method are used to determine parameters α and β [20].

Although the parameterizations of Eq. (1.2) and (1.3) are sensible in terms of estimation through regression analyses, and are not easily interpretable in physical terms. A mathematically equivalent form of the log odds PoD (a) model is given in Eq. 1.4.

$$PoD(a) = \left\{ 1 + \exp - \left[\frac{\pi}{\sqrt{3}} \left(\frac{\ln a - \mu}{\sigma} \right) \right] \right\}^{-1} \quad (1.4)$$

In this form, $\mu = \ln a_{0.5}$, where $a_{0.5}$ is the flaw size that is detected 50% of the time, that is, the median detectable crack size. The steepness of the PoD(a) function is inversely proportional to; that is, the smaller the value of σ , the steeper the PoD(a) function. The parameters of Eq (1.2) and (1.4) are related by Eq. (1.5) and (1.6).

$$\mu = \frac{-\alpha}{\beta} \quad (1.5)$$

$$\sigma = \frac{\pi}{(\beta\sqrt{3})} \quad (1.6)$$

The log odds PoD(a) function is practically equivalent to a cumulative log normal distribution with the same parameters, μ and σ of Eq (1.4). Below figure compares the log odds and cumulative log normal distribution functions for $\mu = 0$ and $\sigma = 1$. Equation (1.4) is the form of the log odds model that will be used in the "Analysis of Hit/Miss Data" [27].

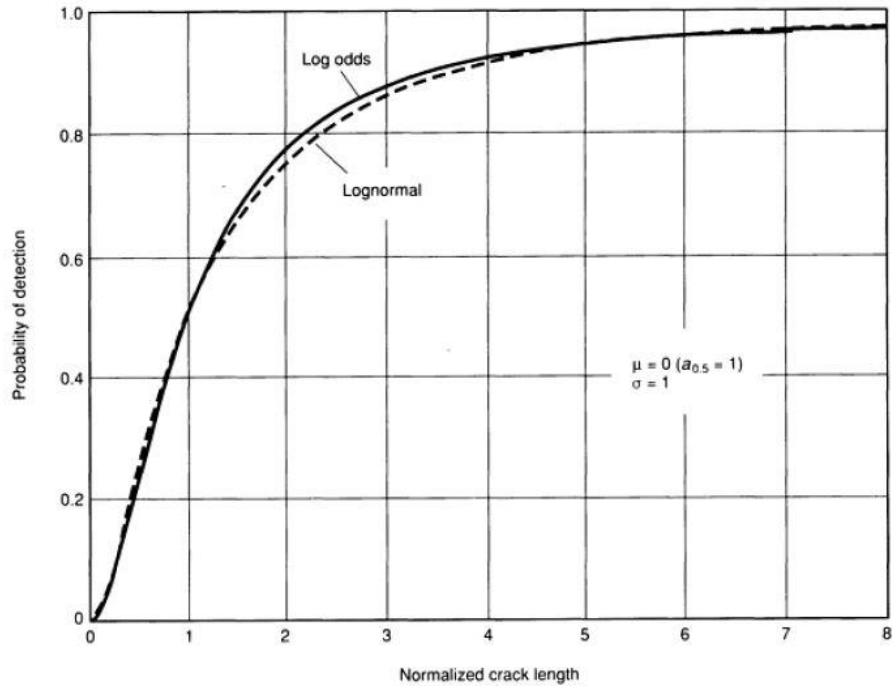


Figure 1.21 Comparison of log odds and cumulative log normal models [27]

1.4.4 PoD (a) Curves from Signal Response Data (\hat{a})

In an eddy current system, a peak voltage can be referenced as a signal response. In fluorescent penetrant testing, the response can be a brightness and/or size of indication. Briefly, in an NDT system, a defect depth or size a is causing a signal response (screen height in UT) which is called as \hat{a} . In signal response system, much more data is supplied than in hit/miss analysis.

The amplitude of the signal \hat{a} to the size a is considered as a random value and is associated with a probability density $g_a(\hat{a})$. The relation between \hat{a} and a can be expressed as;

$$\hat{a} = \mu(a) + \delta \quad (1.7)$$

where $\mu(a)$ is the mean of $g_a(\hat{a})$ and δ is a random error term accounting for the differences between \hat{a} and $\mu(a)$. The distributional properties of δ determine the probability density $g_a(\hat{a})$ about $\mu(a)$.

In practice, it is often assumed that δ is normally distributed with zero mean and a constant variance (independent of a). $g_a(\hat{a})$ is then the normal probability density function with mean $\mu(a) = 0$ and variance equal to that of δ [30].

The Probability of Detection as a function of a , flaw characteristic (size, depth, etc.), can be gained from the relation between \hat{a} and a .

$$PoD(a) = \int_{\hat{a}_{dec}}^{\infty} g_a(\hat{a}) \times d\hat{a} \quad (1.8)$$

Above calculation represents the probability of detection as the shaded area under the density functions can be found in Figure 1.22.

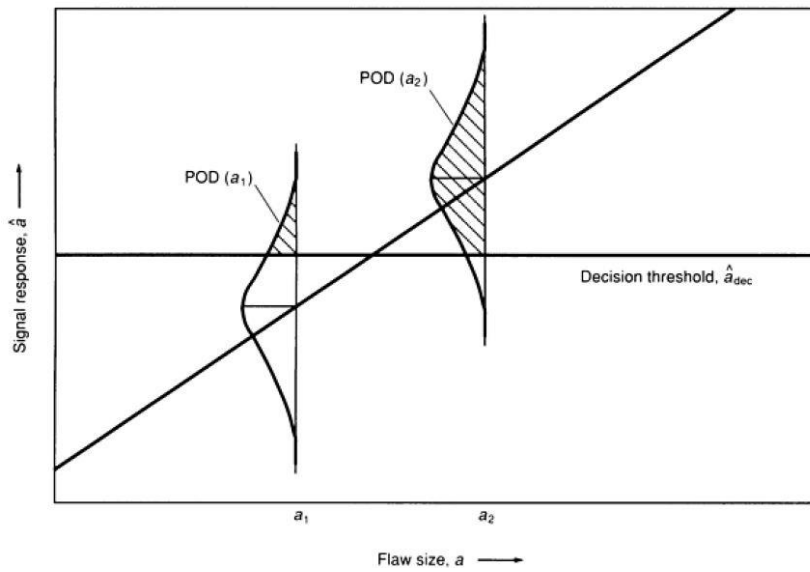


Figure 1.22 PoD (a) calculations from \hat{a} vs a relation [27]

In PoD curves for signal response data, it was determined in several studies that an approximate linear relationship exists between $\ln(\hat{a})$ and $\ln(a)$ [20].

$$\ln(\hat{a}) = \beta_0 + \beta_1 \ln(a) + \delta \quad (1.9)$$

Where, δ an error term which is normally distributed with zero mean and constant standard deviation σ_δ .

The PoD (a) function calculation for \hat{a} data (signal response data) can be expressed as

$$\text{PoD} (a) = \text{Probability} [\hat{a} > \hat{a}_{dec}] \quad (1.10)$$

$$\text{PoD} (a) = \text{Probability} [\ln (\hat{a}) > \ln (\hat{a}_{dec})] \quad (1.11)$$

$$\text{PoD} (a) = 1 - \phi \left[\frac{\ln(\hat{a}_{dec}) - \beta_0 + \beta_1 \ln(a)}{\sigma_\delta} \right] \quad (1.12)$$

Where, ϕ is the standard normal distribution function. Using the symmetry properties of ϕ , equation 1.12 can be written as

$$\text{PoD} (a) = \phi \left[\frac{\ln(a) - [\ln(\hat{a}_{dec}) - \beta_0] / \beta_1}{\sigma_\delta / \beta_1} \right] \quad (1.13)$$

Equation 1.13 is a cumulative log normal distribution function with mean and standard deviation of log signal response given in Equation 1.14 and 1.15

$$\mu = \frac{\ln(\hat{a}_{dec}) - \beta_0}{\beta_1} \quad (1.14)$$

$$\sigma = \frac{\sigma_\delta}{\beta_1} \quad (1.15)$$

In order to calculate the PoD function, the parameters of β_0 , β_1 , and σ_δ need to be calculated from the PoD data by using the maximum likelihood methods [27].

1.4.5 Parameters Affecting Probability of Detection

Some operational and physical parameters should be considered to set up and conduct a PoD demonstration successfully. Most of these below mentioned parameters are applicable to almost all of NDT systems.

Experimental design is one of the important aspects in PoD analysis. The conditions of the NDT inspection parameters determined by the experimental design Establishment of the relationship between the PoD and the signal response data (target size, depth or screen height and etc.) need to be implemented in order to reach the objective of NDT system; not to determine the smallest crack the system can find, to determine the largest crack the system can miss. This defines the capability of NDT system under representative inspection conditions.

Another parameter to have an influence in PoD analysis is the calibration. Calibration is the process of determining the performance indicators of a system by comparing them with measurement standards. Calibration ensures that an NDT system will produce extractions which meet some defined criteria with some degree of confidence, based on analysis of the systems' output and quantified with PoD relationship. An effective calibration produces reliable data which directly affect the PoD reliability. Briefly, an excellent system with poor calibration produces data of no consequence thus no reliable statistical analysis.

Materials properties have influence on system reliability. These can be either particular chemicals for penetrant inspections or grain size values for ultrasonic testing. Beside, residual stresses, part geometry, specimen pre-processing like surface preparations (machining), chemical cleaning or abrasive blasting can be counted as variables effecting test reliability. Each of these variables can have a significant effect on PoD reliability [31].

Concerning effects of material properties to PoD reliability, one example study was performed by Spies et.al. using ferritic-austenitic stainless steel. Duplex steel microstructure causes excessive attenuation of the ultrasonic waves. Thus, in order to determine the improved defect detection, the Synthetic Aperture Focusing Technique (SAFT) which leads to a reduction of the microstructural noise signals was applied. Using SAFT algorithm led to better results which also can be recognized in the plotted PoD curves as well [32].

Specimen and flaws, additionally to above parameters, shouldn't have big differences with the specimen that are being tested by the NDT system in terms of physical characteristics. In PoD analysis, experience suggests that the specimen test set should contain at least 60 targets in binary analysis (hit/miss analysis) and at least 30 targets if the signal response analysis is processed. Additionally, it has been implied that for binary analysis, 120 inspection probabilities will result more precise estimate of a_{50} . For most NDT techniques, the geometric considerations and flaw properties (location and orientation) are also significant variables. Corner flaws versus surface cracks can be given as an example of flaw orientations. In a study made by Kierspel et al, the superiority and reliability of phased array system against conventional ultrasonic system was determined. The measurements were made on aluminum test specimen with groups of artificial flaws. It was determined that the flat bottom holes indication can only be anticipated as a small bulb in front of back wall echo in A-scan image. In opposition to that, phased array technique gives a clear signal from the back wall as well as defined indication of artificially created flaws. Moreover, neither physical movement nor any exchanging of the probe wedge was required. As a result, the superiority of phased array compared to conventional ultrasonic testing was determined when the flaw location is close to the back wall. Also it was monitored that the multiple angle inspection can improve the PoD when there is limited access to an inspection surface [33].

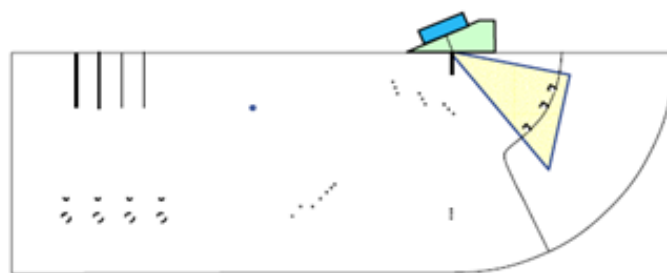


Figure 1.23 Resolution before back wall (2 and 4 mm FBH) [33]



Figure 1.24 Results for the resolution before back wall FBHs. (left: conventional ultrasonic, right: phased array) [33]

Another study was made in order to model the defects that resemble in-service inspections and to create PoD curves of these defects. Most of the defects are created by EDM notches resulted in smooth contours in ultrasonic simulations. However, defects found in in-service inspections may have different shape, rough surfaces, tilt and skew. All these parameters may cause scattering of the ultrasound. Measurements were simulated with using rough, tilted and skewed artificial flaws using angular conventional ultrasonic probe. It was observed that roughness affects the detection probability more than tilt and skew [34].

In many Probability of Detection analyses, human factor is accepted as the most significant variable. It's very crucial to implement several adequate inspectors or operators to conduct the inspections for a specific PoD analysis. The selected operators should have the proper training, certification and physical ability [31]. The human reliability factor has been researching extensively and some cases were particularly identified in literature. For example in Figure 1.25, the human reliability was illustrated for inspection of titanium plates having low cycle fatigue cracks by ultrasonic immersion test.

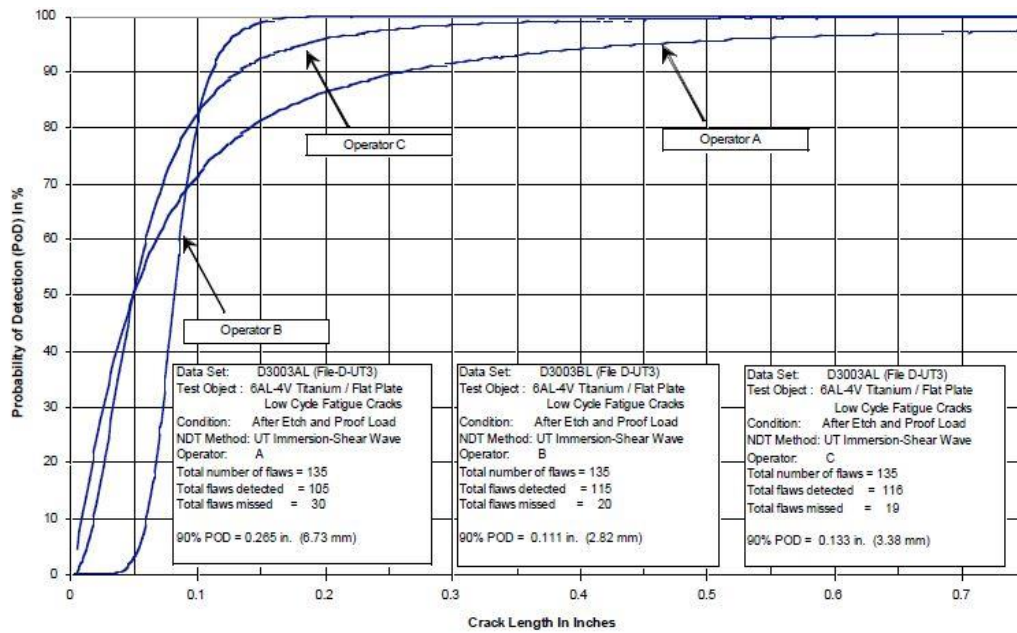


Figure 1.25 PoD model results for UT: Different operators inspecting same specimen [20]

In summary, there are several important operational and physical parameters which have significant effects on Probability of Detection (PoD) analyses such as NDT method, calibration of system and equipment, chemical components, material properties, surface conditions, flaw characteristics and etc. The design of PoD study should be engineered with considering all aspects with comparing the real inspection conditions.

CHAPTER 2

EXPERIMENTAL PROCEDURE

2.1 Material Selection and Properties

Various types of steels are used for different applications with considering their mechanical and chemical properties.

Metals, as known, may have many alloying variations. Metal grain structure can be varied by alloy, heat treatment and etc. All these factors will provide differences in the result of ultrasonic test manifested as variations in velocity and attenuation [35]. Put another way, the internal structure of material has a considerable effect on test results of ultrasonic based inspection methods.

In this study, 3 types of steels that are widely used in industry were selected;

- Plain Carbon steel / St-37 (DIN 17100)
- Low - Alloyed Steel / 42CrMo4 (SAE 4140)
- High – Alloyed Steel / SAE 316 L

Plain carbon steel is the also known as Mild Steel, is the most used and common form of steel because its price is relatively low while it provides mechanical properties that are acceptable for many applications. Low-carbon steel contains approximately 0.05–0.320% carbon making it malleable and ductile. Mild steel has a relatively low tensile strength, but it is cheap and malleable; surface hardness can be increased through carburizing. It is often used when large quantities of steel are needed, for example as structural steel [36].

The St-37 sample was taken from a hot rolled product and chemical composition and micrograph given in Table 2.1 and Figure 2.1.

Table 2.1 Chemical composition of St-37steel [37].

	C	Si	Mn	P	S	N	Cu	CEV
%	0.02	-	1.4	0.035	0.035	0.012	0.55	0.38



Figure 2.1 Representative micrograph of the St-37 specimen.

In alloyed steels, various elements are used to improve the mechanical properties of steels in total amounts between 1 % and 50 % by weight. They are generally grouped into two; low-alloy steels and high-alloy steels. The difference between these two groups are the alloying elements content which is 4.0 % [38].

SAE Grade 42CrMo4 was selected low-alloyed steel specimen. The 42CrMo4 steels are defined as alloyed heat treatable steel / chromoly steel with a typical tensile strength of 900 - 1200 N/mm². These grades are known with their excellent strength to ratio which makes this grade as HSLA steel. This steel grade is widely used as push rods, gears, and axle journals in aircraft components and automotive industry with their high toughness property.

Table 2.2 Chemical composition of SAE 4140 steel

	C	Si	Mn	P	S	Cr	Mo
%	0.38-0.45	Max. 0.4	0.6-0.9	0.035	0.035	0.9-1.2	0.15-0.3



Figure 2.2 Representative micrograph of the 42CrMo4 (SAE 4140) specimen.

Stainless steels are described as High – Alloyed steels in literature. Most of the stainless steels have good corrosion resistance in standard atmospheric conditions, in most of the aqueous media and in oxidizing acids such as nitric acid. Various compositional modifications are applied to the stainless steels for enhancing the corrosion resistance of them for specific applications [39]. SAE 316 L grade austenitic stainless steel was chosen due to its wide range of industry usage.

Table 2.3 Chemical composition of SAE 316 L steel

	C	Si	Mn	Ni	P	S	Cr	Mo
%	Max 0.03	Max 1	Max 2	10.5-13	Max 0.045	Max 0.015	16.5-18.5	2.5-3



Figure 2.3 Representative micrograph of the SAE 316L specimen (x100)

For the three types of steels microstructural analysis and grain size measurements were done using image analysis software, in order to evaluate the effect of grain sizes on inspection system.

2.2 Sample Preparation

Two types of specimens were prepared for the inspection purposes. These specimens which bought for the experiments were prepared / manufactured with using CNC vertical lathe and Electrical discharge machine (EDM).

2.2.1 Specimen Type 1

In the specimen type 1, 10 artificial flaws with 2 mm diameter were created at different depths in St-37 specimen. The solid part of test specimen was drawn in Solid Edge software in and using Edge Cam software, the allocation of required cutting tools and design of drilling operation was performed. Following to that, as per solid drawings, the flaws were drilled with CNC vertical lathe in different depths.

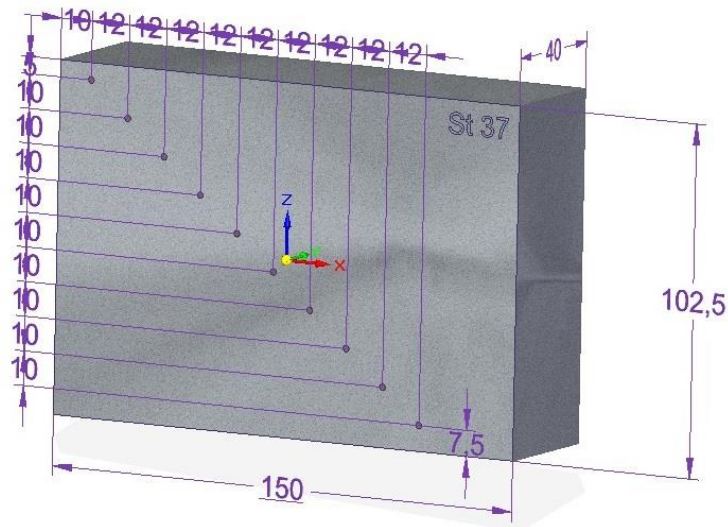


Figure 2.4 Schematic view of the specimen type 1



Figure 2.5 Type 1 specimen preparations with CNC vertical lathe

2.2.2 Specimen Type 2

In the specimen type 2, 10 artificial flaws which have different diameters were created at the same depths (60 mm) by using Electrical Discharge Machining (EDM).

Electrical discharge machining (EDM) is a non- conventional material removal processes and extensively used in industry. The initial applications of EDM can be seen in 1770s, when English chemist Joseph Priestly discovered the erosive effect of sparks and electrical discharges. However in 1943, the electrical discharges destructive properties for constructive use exploited in Moscow University.

The process of material erosion mechanism initiated in a dielectric fluid between the electrode and workpiece by conversion of electrical energy into thermal energy through a series of discrete electrical discharges. This resulted as a created plasma channel in a range of 8000 to 12000°C between cathode and anode initializing a substantial amount of heating and melting of material at the surface of each pole. The EDM system is named as non-conventional removal process because of the

removal of material using the melting and evaporation of material from the workpiece surface is not mechanical. The volume of material removed per discharge is typically in the range of $10^{-6} - 10^{-4} \text{ mm}^3$ and the material remove rate is usually between 2 and 400 mm^3/min [40] depending on specific application [41].

The EDM process's ability to shape difficult material with high precision gives the privilege to the system in industry. Any conductive materials can be machined regardless of its hardness and also there is no mechanical stresses are created in the workpiece. Small hole drilling possibility with diameters as small as 0.2 is also an advantage against other manufacturing processes.

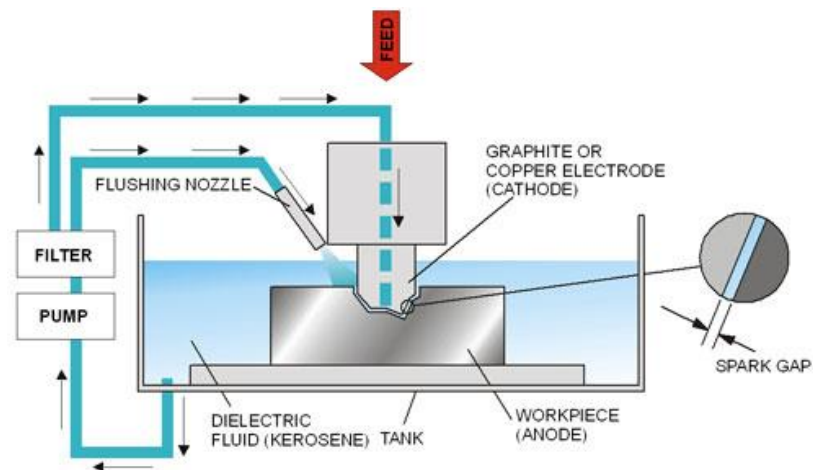


Figure 2.6 The basic principle of Electrical Discharge Machining



Figure 2.7 Hole drilling with using Electrical Discharge Machining

Flaws bigger than 3 mm in diameter were initially created with using EDM and hydraulic drilling machine with a HSS drill bits were used afterwards to reach up to bigger diameters. Figure 2.8 shows the artificial flaws created in different diameters.

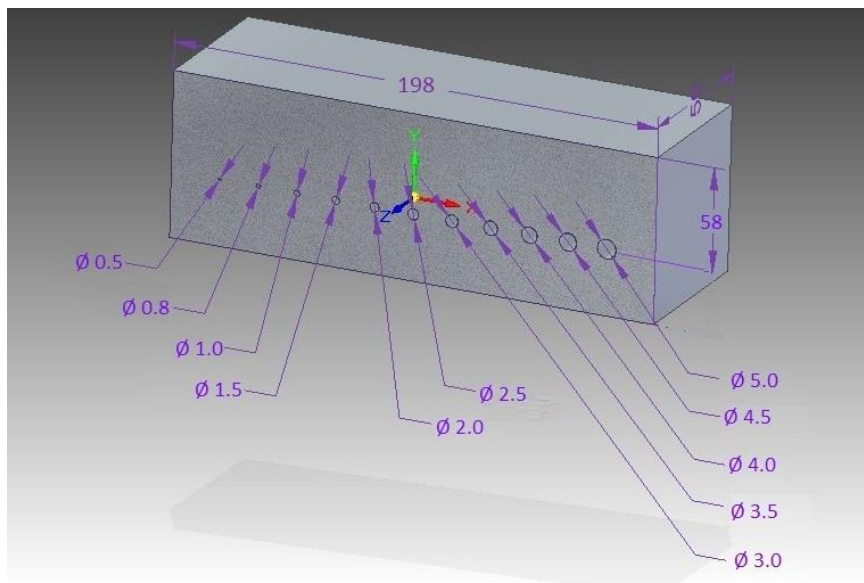


Figure 2.8 Schematic view of the specimen type 2

As known from the literature, the surface condition is an important measure that has to be taken into account when an ultrasonic testing should be done. As mentioned in literature, there is no directly proportional relation between ultrasonic signal amplitude reduction and increasing surface roughness. Hence, because of the insufficient coupling condition due to surface roughness, ultrasonic signal reduction follows an exponentially decreasing path. As a result increased surface roughness can decrease the transmitted sound pressure which can cause reduction of ultrasonic signals when the echo height is important measure for the test [35].

Considering above mentioned reasons, all specimen inspection surface was grinded in the same conditions with a low roughness in METU / MetE Mechanical workshop.

2.3 Metallographic Investigations

Non-Destructive Testing Techniques are using to determine the presence or absence of flaws in the component. If the flaw exists, then it is characterized with respect to location, size, orientation, shape, nature, etc. to determine its acceptability under the operating conditions.

In assessing the structural integrity of a component, the material property is as important as flaw characteristics. One of the most used NDT technique for characterization of material properties is Ultrasonic testing. Ultrasonic testing parameters are significantly affected by changes in microstructural or mechanical properties of materials.

Some of the important material and metallurgical properties like elastic modulus, fracture toughness, yield strength, hardness, grain size, inclusion content and etc have been correlated with ultrasonic testing parameters.

Attenuation refers to the loss of sound energy as the ultrasonic beam passes through the material. Attenuation has two components, absorption and scattering. Energy

loss due to absorption is a result of mechanisms such as dislocation damping, hysteresis losses, thermoelastic effects, etc. Loss due to scattering in polycrystalline materials depend on the ratio of grain size (D) and wavelength (λ) [42].

It has been studied that the ultrasound velocity is directly influenced by the microstructural phases of steel. An inverse relationship between ultrasonic velocity and hardness of the heat treated steel specimens. Microstructure having the highest hardness is the one having the lowest ultrasonic velocity and vice versa. It was determined that the most attenuating phases are martensite and coarse pearlite, and the least attenuating phases are bainite and martensite tempered at 600°C [43].

Specimens selected for this thesis were investigated in terms of microstructure / grain sizes. Grain size numbers were calculated as per ASTM E 1382 by intercept method. Results of grain sizes are 7.38 for St-37, 8.20 for 4140 and 8.12 for 316 L respectively. As a result, it was determined that the grain sizes of selected materials show no deviances and their effects to the test are negligible.

2.4 Ultrasonic Inspections

Krautkramer Branson USD 15 and Sonotron Isonic UT Pod in conventional ultrasonic mode equipment were used for ultrasonic inspections at METU Welding Technology and Non – Destructive Testing Research / Application Center. The 4 MHz contact type probe was used. The machine oil was used as a couplant for all inspections.

The data retrieved from the equipment for the Probability of Detection (PoD) analysis were the screen height values received from the artificially created flaws.

Data retrieved from tests are given in Table 2.4 to Table 2.7.

Table 2.4 Data retrieved from specimen type 1 by ultrasonic method
(for the flaws 2 mm in diameter located at different depths)

ID	Sound path (mm)	Screen height (%)	Remaining screen height (%)	ID	Sound path (mm)	Screen height (%)	Remaining screen height (%)
1	14,2	99	1	18	14,4	98	2
2	24,1	87,9	12,1	19	24,1	85	15
3	34,1	68	32	20	34,5	63	37
4	44,1	50,4	49,6	21	44,5	46,5	53,5
5	53,6	39,1	60,9	22	54,3	37	63
6	63,5	32	68	23	64,2	28	72
7	73,5	28,1	71,9	24	74,3	23	77
8	83,4	23,8	76,2	25	84,3	20	80
9	93,4	16,8	83,2	26	94,4	18	82
10	21,7	92	8	27	21,9	93	7
11	31,6	73	27	28	31,8	73	27
12	41,6	60	40	29	41,7	48	52
13	51,4	40	60	30	51,7	41	59
14	61,4	37	63	31	61,5	33	67
15	71,4	29	71	32	71,8	25	75
16	81,3	26,5	73,5	33	81,8	23	77
17	91,6	21	79	34	91,5	20	80

Table 2.5 Data retrieved from St-37 specimen by ultrasonic method

ID	Flaw Size (mm)	Screen height (%)	Remaining screen Height (%)	ID	Flaw Size (mm)	Screen height (%)	Remaining screen Height (%)
1	5	99	1	18	2	50	50
2	4,5	96	4	19	1,5	47	53
3	4	76	24	20	1	47	53
4	3,5	53	47	21	0,8	46	54
5	3	65	35	22	0,5	39	61
6	2,5	50	50	23	5	99	1
7	2	45	55	24	4,5	90	10
8	1,5	43	57	25	4	75	25
9	1	45	55	26	3,5	63	37
10	0,8	40	60	27	3	65	35
11	0,5	48	52	28	2,5	53	47
12	5	99	1	29	2	48	52
13	4,5	85	15	30	1,5	46	54
14	4	73	27	31	1	43	57
15	3,5	58	42	32	0,8	42	58
16	3	66	34	33	0,5	36	64
17	2,5	54	46				

Table 2.6 Data retrieved from SAE 4140 specimen by ultrasonic method

ID	Flaw Size (mm)	Screen height (%)	Remaining screen Height (%)	ID	Flaw Size (mm)	Screen height (%)	Remaining screen Height (%)
1	5	99	1	18	2	62	38
2	4,5	95	5	19	1,5	55	45
3	4	89	11	20	1	50	50
4	3,5	80	20	21	0,8	42	58
5	3	78	22	22	0,5	36	64
6	2,5	75	25	23	5	99	1
7	2	67	33	24	4,5	96	4
8	1,5	60	40	25	4	82	18
9	1	52	48	26	3,5	81	19
10	0,8	51	49	27	3	79	21
11	0,5	44	56	28	2,5	77	23
12	5	99	1	29	2	75	25
13	4,5	95	5	30	1,5	65	35
14	4	85	15	31	1	58	42
15	3,5	85	15	32	0,8	49	51
16	3	75	25	33	0,5	41	59
17	2,5	70	30				

Table 2.7 Data retrieved from SAE 316 L specimen by ultrasonic method

ID	Flaw Size (mm)	Screen height (%)	Remaining screen Height (%)	ID	Flaw Size (mm)	Screen height (%)	Remaining screen Height (%)
1	5	99	1	18	2	64	36
2	4,5	98	2	19	1,5	53	47
3	4	84	16	20	1	48	52
4	3,5	79	21	21	0,8	40	60
5	3	76	24	22	0,5	29	71
6	2,5	69	31	23	5	99	1
7	2	67	33	24	4,5	98	2
8	1,5	58	42	25	4	91	9
9	1	50	50	26	3,5	83	17
10	0,8	32	68	27	3	75	25
11	0,5	31	69	28	2,5	71	29
12	5	99	1	29	2	65	35
13	4,5	96	4	30	1,5	56	44
14	4	95	5	31	1	49	51
15	3,5	89	11	32	0,8	36	64
16	3	76	24	33	0,5	30	70
17	2,5	72	28				

2.5 Phased Array Inspections

Sonotron Isonic 2010 phased array equipment was used for ultrasonic inspections, and all inspections were performed at Metu NDT Center. The phased array linear probe with 32 apertures was used in inspections. Distances of flaws from inspection surface were adjusted into the inspection system from “focal depth” setup. In order to eliminate roughness of surface’s effect, the machine oil was used as a couplant in all inspections.

The data retrieved from the equipment for the Probability of Detection (PoD) analysis were the screen height values received from the artificially created flaws which can be found in Table 2.8 to Table 2.11.

Table 2.8 Data retrieved from specimen type 1 by phased array method
(for the flaws 2 mm in diameter located at different depths)

ID	Sound path (mm)	Screen height (%)	Remaining screen Height (%)	ID	Sound path (mm)	Screen height (%)	Remaining screen Height (%)
1	14,2	99	1	18	14,4	98	2
2	24,1	73	27	19	24,1	77	23
3	34,1	59	41	20	34,5	62	38
4	44,1	44	56	21	44,5	50,5	49,5
5	53,6	36	64	22	54,3	41,5	58,5
6	63,5	29	71	23	64,2	32,5	67,5
7	73,5	27,5	72,5	24	74,3	30	70
8	83,4	21	79	25	84,3	25	75
9	93,4	19	81	26	94,4	20	80
10	21,7	81	19	27	21,9	96	4
11	31,6	61	39	28	31,8	68	32
12	41,6	45	55	29	41,7	55	45
13	51,4	39	61	30	51,7	45	55
14	61,4	32,5	67,5	31	61,5	36	64
15	71,4	29	71	32	71,8	34	66
16	81,3	25	75	33	81,8	29	71
17	91,6	20,5	79,5	34	91,5	27	73

Table 2.9 Data retrieved from St-37 specimen by phased array method

ID	Flaw Size (mm)	Screen height (%)	Remaining screen Height (%)	ID	Flaw Size (mm)	Screen height (%)	Remaining screen Height (%)
1	5	99	1	18	2	55	45
2	4,5	99	1	19	1,5	50	50
3	4	90	10	20	1	45	55
4	3,5	52	48	21	0,8	43	57
5	3	72	28	22	0,5	38	62
6	2,5	56	44	23	5	99	1
7	2	43	57	24	4,5	95	5
8	1,5	50	50	25	4	85	15
9	1	52	48	26	3,5	75	25
10	0,8	50	50	27	3	72	28
11	0,5	42	58	28	2,5	65	35
12	5	99	1	29	2	55	45
13	4,5	95	5	30	1,5	50	50
14	4	73	27	31	1	48	52
15	3,5	67	33	32	0,8	46	54
16	3	70	30	33	0,5	39	61
17	2,5	60	40				

Table 2.10 Data retrieved from SAE 4140 specimen by phased array method

ID	Flaw Size (mm)	Screen height (%)	Remaining screen Height (%)	ID	Flaw Size (mm)	Screen height (%)	Remaining screen Height (%)
1	5	99	1	18	2	66	34
2	4,5	97	3	19	1,5	55	45
3	4	95	5	20	1	47	53
4	3,5	86	14	21	0,8	43	57
5	3	84	16	22	0,5	38	62
6	2,5	83	17	23	5	98	2
7	2	68	32	24	4,5	95	5
8	1,5	60	40	25	4	92	8
9	1	51	49	26	3,5	80	20
10	0,8	42	58	27	3	78	22
11	0,5	41	59	28	2,5	76	24
12	5	98	2	29	2	67	33
13	4,5	90	10	30	1,5	58	42
14	4	87	13	31	1	49	51
15	3,5	76	24	32	0,8	43	57
16	3	75	25	33	0,5	39	61
17	2,5	70	30				

Table 2.11 Data retrieved from SAE 316 L specimen by phased array method

ID	Flaw Size (mm)	Screen height (%)	Remaining screen Height (%)	ID	Flaw Size (mm)	Screen height (%)	Remaining screen Height (%)
1	5	99	1	18	2	62	38
2	4,5	90	10	19	1,5	54	46
3	4	86	14	20	1	46	54
4	3,5	80	20	21	0,8	43	57
5	3	74	26	22	0,5	36	64
6	2,5	74	26	23	5	99	1
7	2	60	40	24	4,5	93	7
8	1,5	48	52	25	4	85	15
9	1	43	57	26	3,5	79	21
10	0,8	37	63	27	3	76	24
11	0,5	31	69	28	2,5	73	27
12	5	99	1	29	2	61	39
13	4,5	96	4	30	1,5	51	49
14	4	84	16	31	1	44	56
15	3,5	78	22	32	0,8	40	60
16	3	77	23	33	0,5	35	65
17	2,5	72	28				

2.6 Probability of Detection Analysis

Probability of Detection analyses of inspection results was processed with using mh1823 software [44].

For analyzing reliability of NDT, two probabilistic methods are existing and used for producing PoD curves as functions of flaw properties. First, in “hit/miss” data, NDT results were recorded in terms of whether the flaw was detected or not. This reliability method is appropriate for dye-penetrant testing or magnetic particle testing. However, in many NDT systems, unlike binary response, there is more information in the NDT response like peak voltage in eddy current system or signal amplitude in ultrasonic system. Since the NDT signal response can be interpreted as the selected flaw property, the data is called \hat{a} data (i.e. “a hat data”) or “signal response” data [20].

In this study, PoD curves were created with using signal responses and derived from the correlation of “ a vs \hat{a} ” data. The results of inspections were processed with using mh1823 software [44] and PoD curves were obtained.

CHAPTER 3

RESULTS & DISCUSSION

3.1 a vs \hat{a} Model Selection for PoD Analysis

All data retrieved from the inspection records were plotted in 4 different modes. In order to determine the best model for the PoD analysis, model which represents the data as a straight line and approximate constant variance were selected for further analysis.

3.1.1 a vs \hat{a} Models for Type 1 Specimen

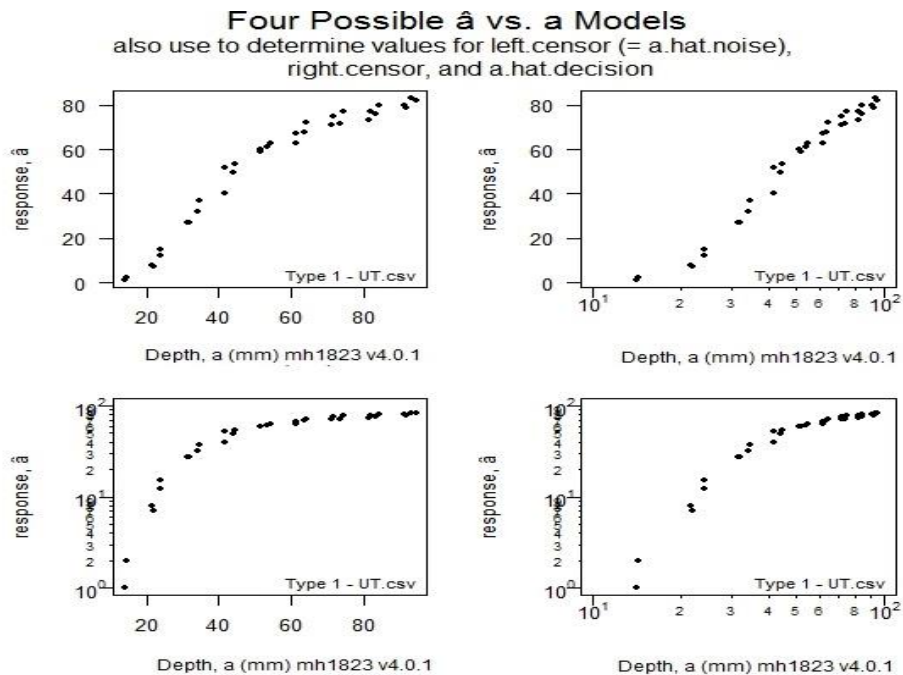


Figure 3.1 Four possible a vs \hat{a} models for Type 1 UT specimen

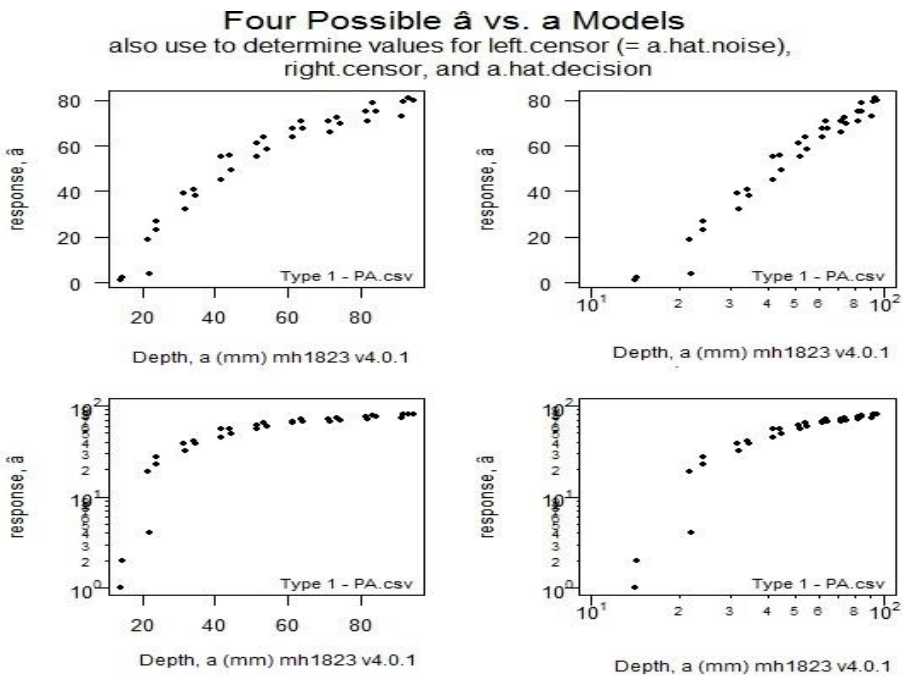


Figure 3.2 Four possible a vs \hat{a} models for Type 1 Phased Array specimen

3.1.2 a vs \hat{a} Models for Type 2 Specimen

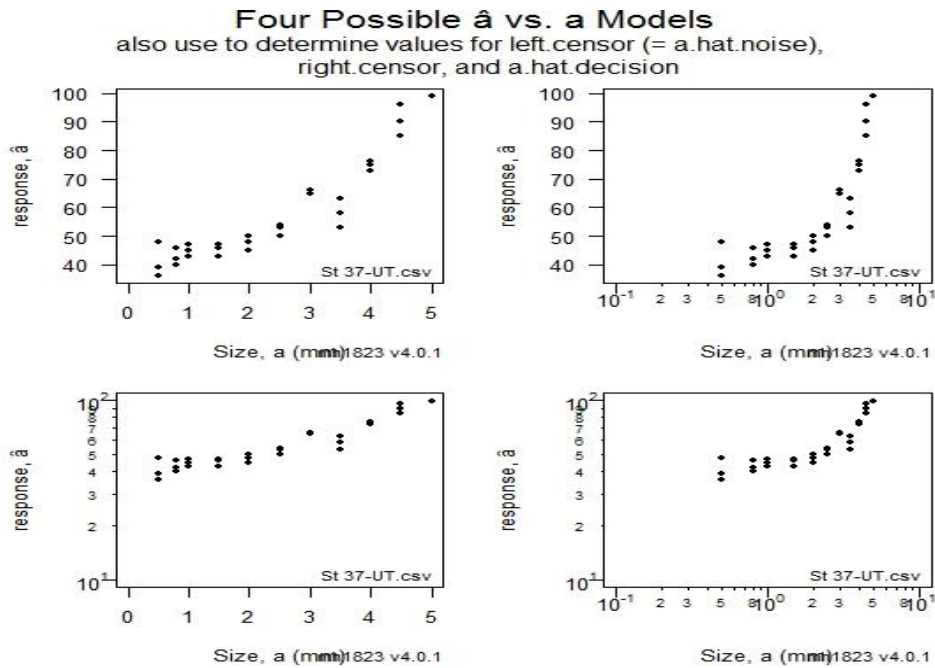


Figure 3.3 Four possible a vs \hat{a} models for Type 2 / St-37 UT specimen

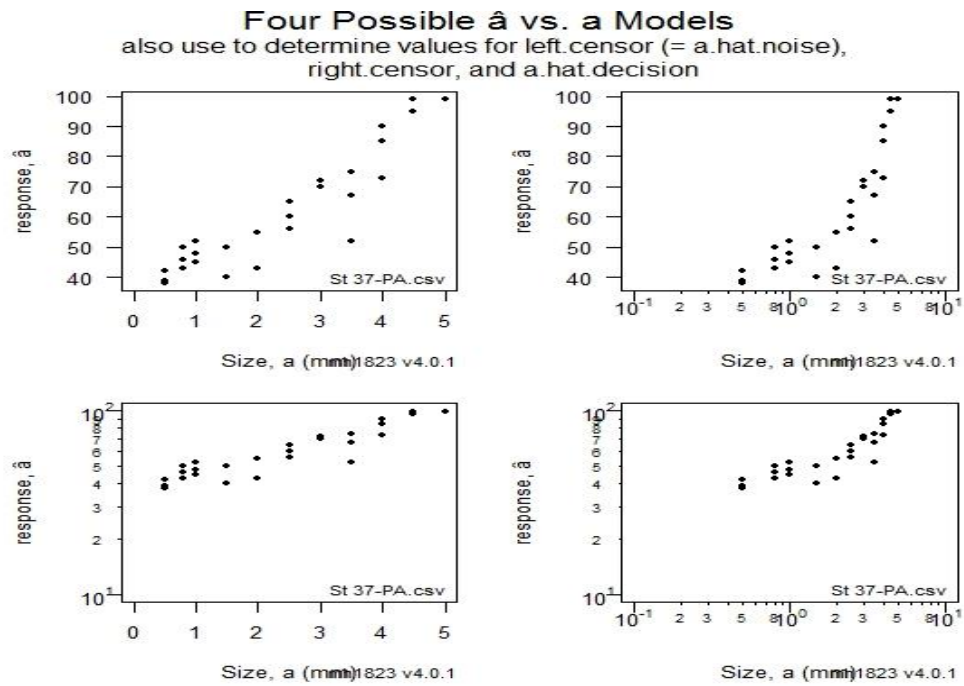


Figure 3.4 Four possible a vs \hat{a} models for Type 2 / St-37 PA specimen

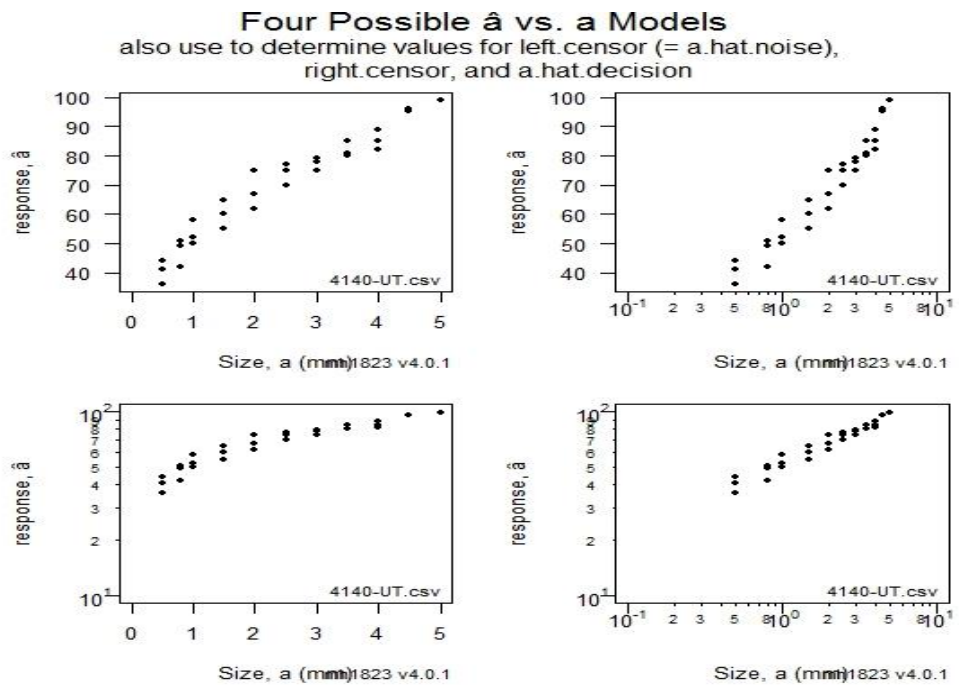


Figure 3.5 Four possible a vs \hat{a} models for Type 2 / SAE 4140 UT specimen

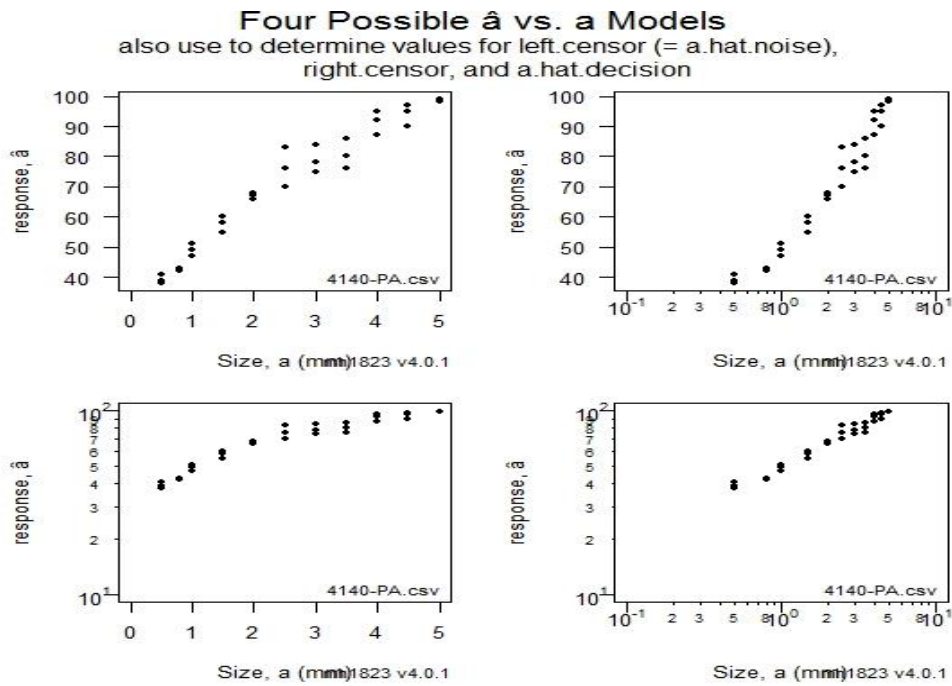


Figure 3.6 Four possible a vs \hat{a} models for Type 2 / SAE 4140 PA specimen

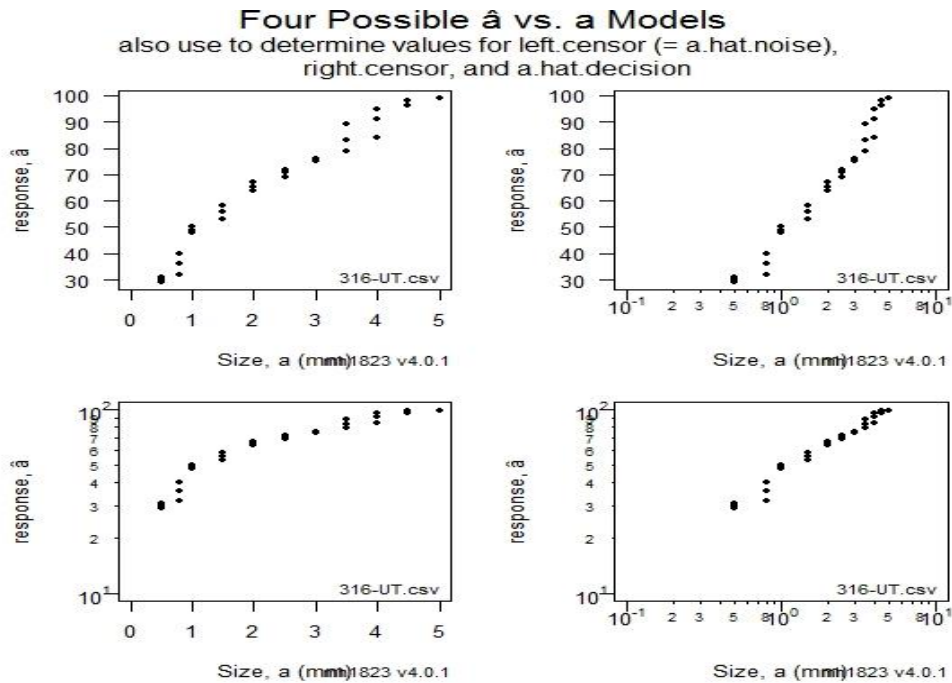


Figure 3.7 Four possible a vs \hat{a} models for Type 2 / SAE 316 UT specimen

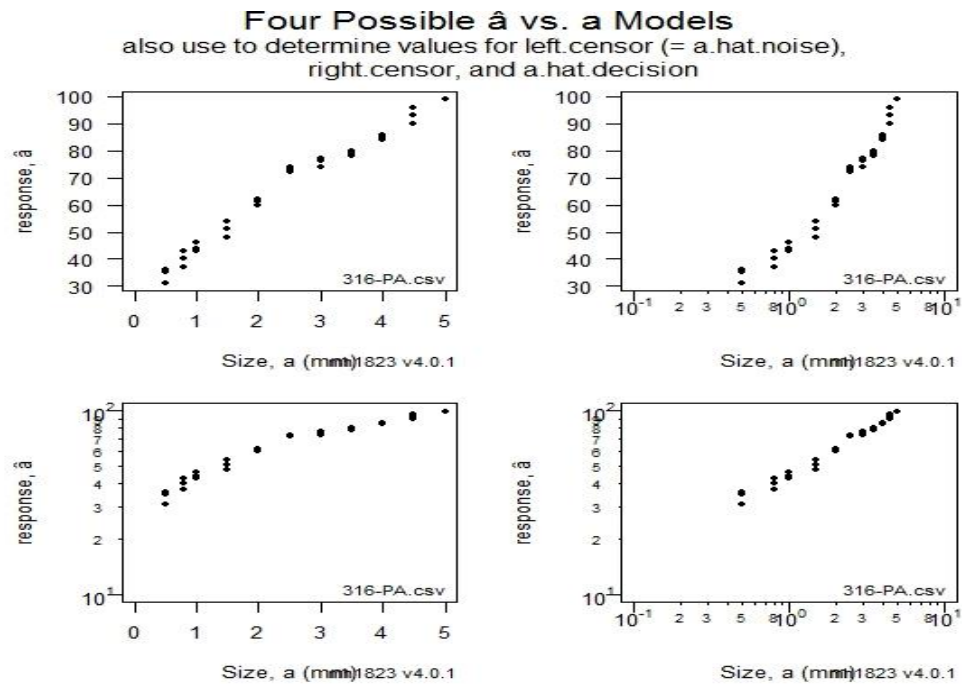


Figure 3.8 Four possible a vs \hat{a} models for Type 2 / SAE 316 UT specimen

3.2 a vs \hat{a} Linear Model Determination for PoD Analysis

After selection of the best representing model, censoring values are determined. All a vs \hat{a} systems have two censoring values. A target's signal that is indistinguishable from the background noise is left censored. The right censoring value corresponds to the maximum possible signal, e.g 100 % screen height. Targets whose responses are censored either on the left or right cannot be described using ordinary least-squares regression and thus need special attention.

In addition to above values, inspection threshold (\hat{a}_{th}) and decision threshold (\hat{a}_{dec}) values also have significant effect of PoD analysis. Inspection threshold is the smallest value of \hat{a} that the system records; the value of \hat{a} below which the signal is indistinguishable from noise. On the other hand, decision threshold is the value of \hat{a} above which the signal is interpreted as a hit, and below which the signal is interpreted as a miss. It is the \hat{a} value associated with 50 % PoD. Decision threshold is always greater than or equal to inspection threshold [31].

Following to selection of best model for all representations, “ \hat{a} decision, left censor, right censor and etc.” choices were selected.

3.2.1 a vs \hat{a} Linear Model for Type 1 Specimen

In type 1 specimen study, both for UT and PA inspections, left censor is determined as 1 and right censor is 100. On the other hand, for UT inspections, \hat{a} decision value is determined as 15 which is the remaining screen height from artificial flaw that located at the end of near field zone. Hence in PA, \hat{a} decision is given as 1 because the focal depth values for PA system can be adapted to the flaw distance to the inspection surface.



Figure 3.9 a vs \hat{a} parameter inputs for UT specimen (left) and Phased Array specimen (right)

Building a vs \hat{a} linear models, confidence and prediction bounds were achieved in mh1823 [44].

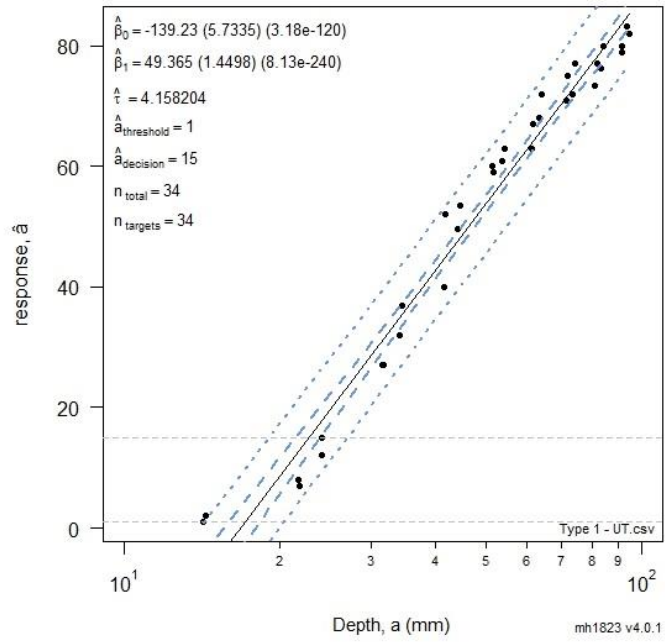


Figure 3.10 a vs \hat{a} linear models of UT Type 1 specimen

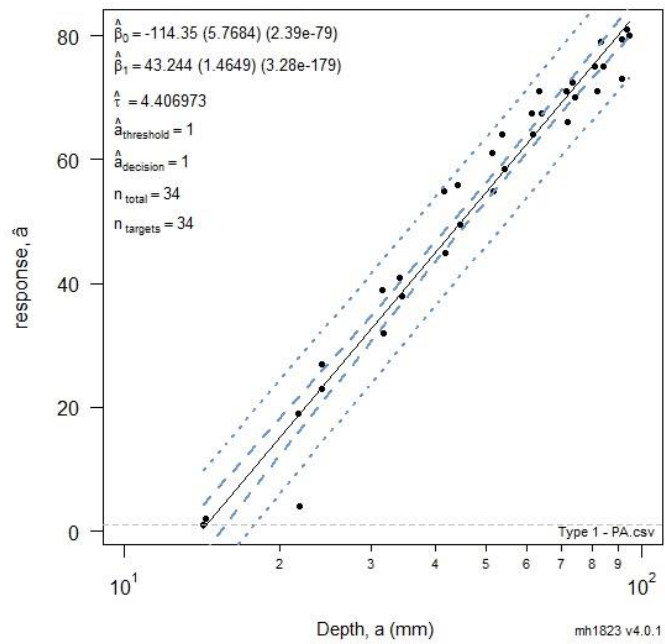


Figure 3.11 a vs \hat{a} linear models of Phased Array Type 1 specimen

3.2.2 a vs \hat{a} Linear Model for Type 2 Specimen

In type 2 specimen studies, both for UT and PA inspections in all material types (ST 37, 4140 and 316), left censor and \hat{a} decision values were described as 25 which is the minimum screen height value determined in the inspections. Right censor value was determined as 100 screen height.

Building a vs \hat{a} linear models, confidence and prediction bounds were achieved in mh1823 for all type of specimen [44].

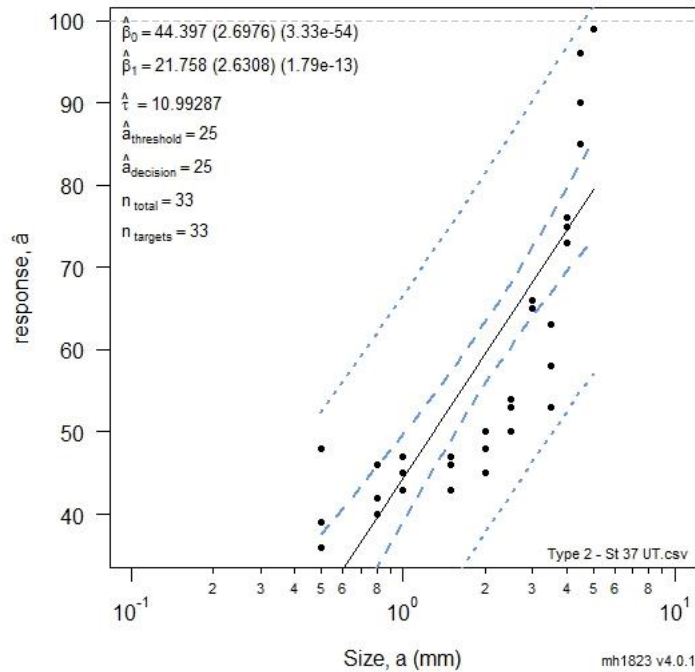


Figure 3.12 a vs \hat{a} linear models of Type 2 / St-37 specimen (UT)

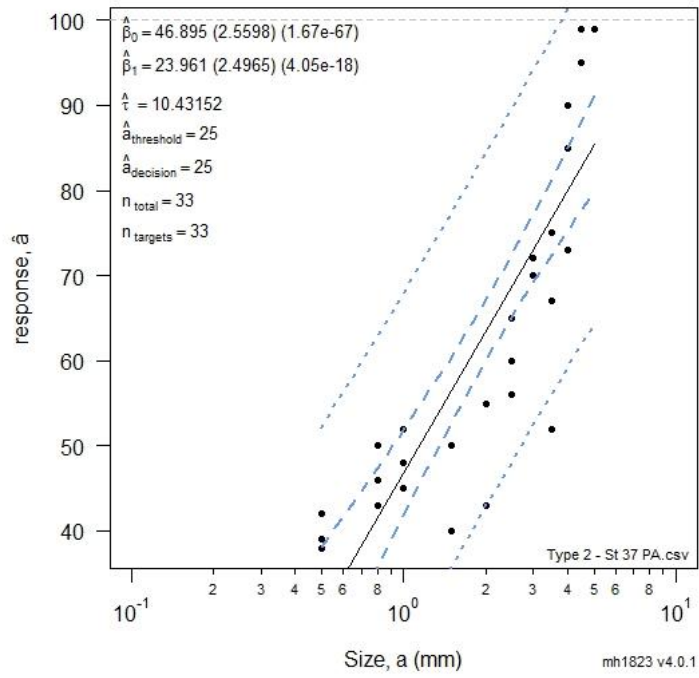


Figure 3.13 a vs \hat{a} linear models of Type 2 / St-37 specimen (PA)

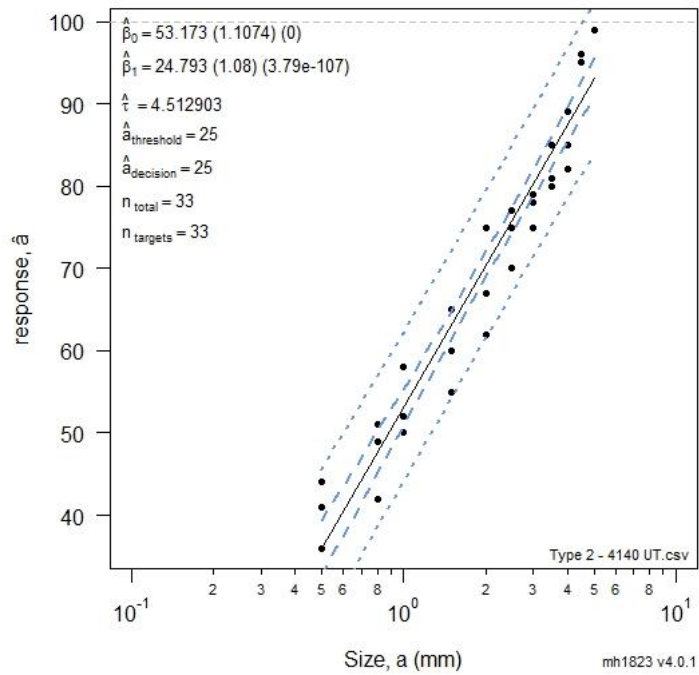


Figure 3.14 a vs \hat{a} linear models of Type 2 / SAE 4140 specimen (UT)

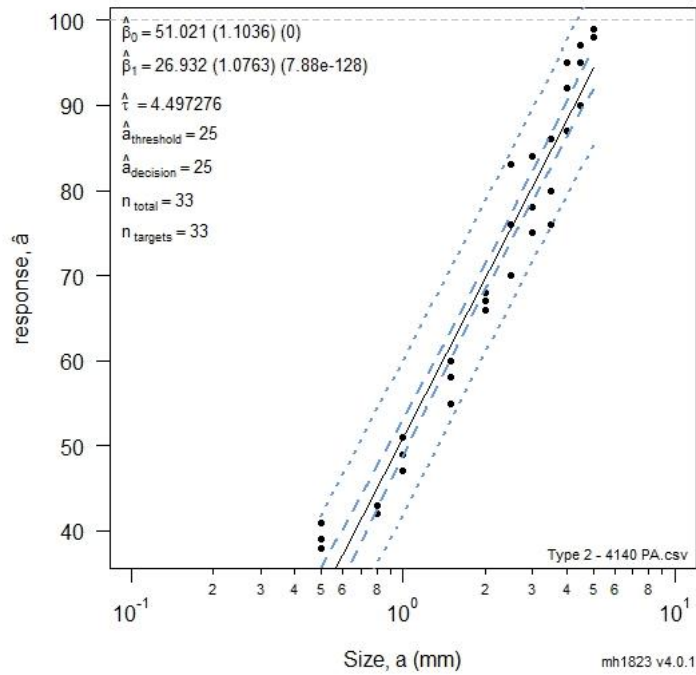


Figure 3.15 a vs \hat{a} linear models of Type 2 / SAE 4140 specimen (PA)

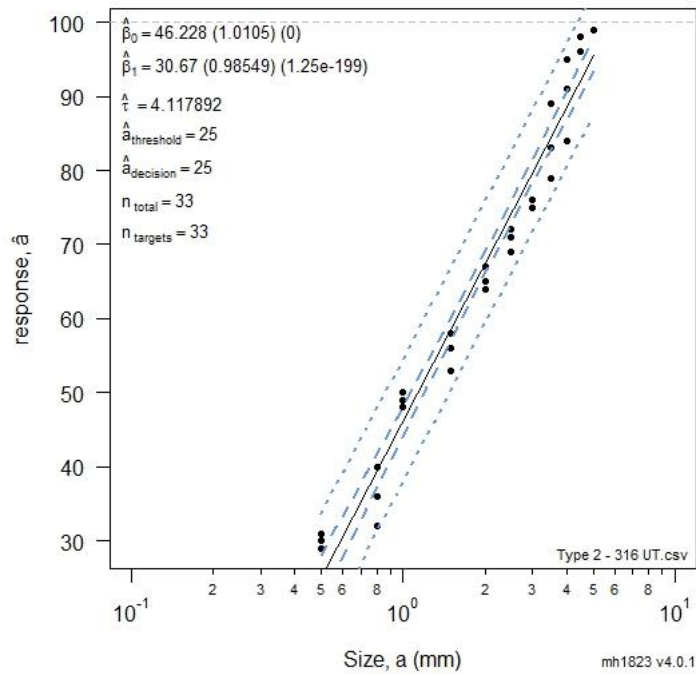


Figure 3.16 a vs \hat{a} linear models of Type 2 / SAE 316 L specimen (UT)

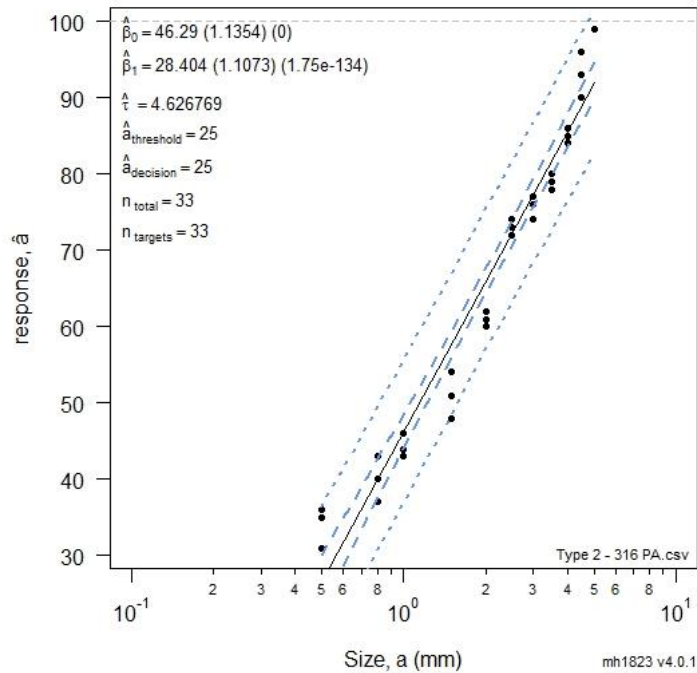


Figure 3.17 a vs \hat{a} linear models of Type 2 / SAE 316 L specimen (PA)

Received data from ultrasonic and phased array systems were processed using mh1823 software [44] to determine the PoD curves. Representing all data received in “ a vs \hat{a} ”, “ $\log(a)$ vs $\log(\hat{a})$ ”, “ a vs $\log(\hat{a})$ ”, “ $\log(a)$ vs \hat{a} ” in plots (Figure 3.1 – 3.8) was the first step of analyze. The data showing a linear behavior was selected as the best model. Then, a vs \hat{a} linear models which show linear approximation of inspection data with the prediction and confidence bounds, inspection threshold (\hat{a}_{th}) and decision threshold (\hat{a}_{dec}), left and right censor thresholds were plotted (Figure 3.9 – 3.17). Finally, the PoD vs. a (depth in type 1, size in Type 2 specimen) graphs are plotted and 50 % Probability of Detection of flaw (a_{50}), 90 % Probability of Detection of flaw (a_{90}) and 90 % Probability of Detection of flaw with a confidence interval of 95 % of a flaw ($a_{90/95}$) sizes were obtained (Figure 3.18 – 3. 25).

3.3 Type 1 Specimen PoD Analysis

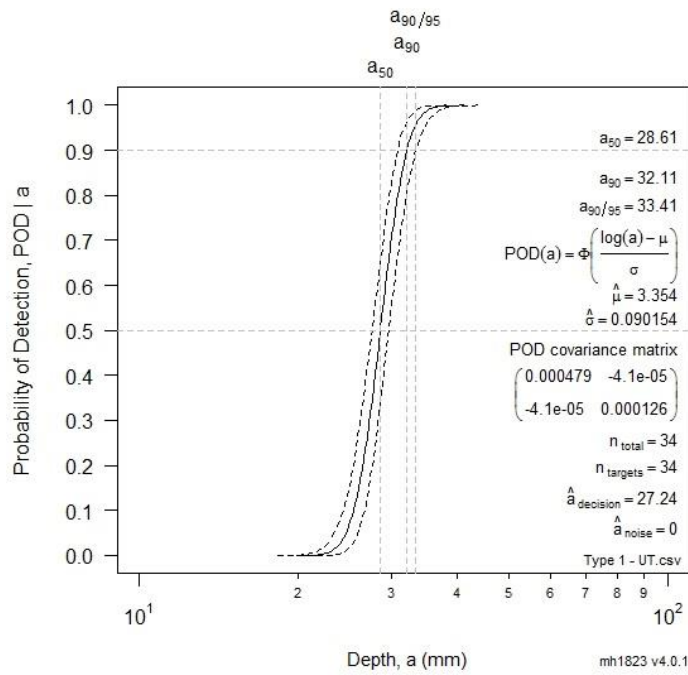


Figure 3.18 PoD curve of Type 1 specimen (UT)

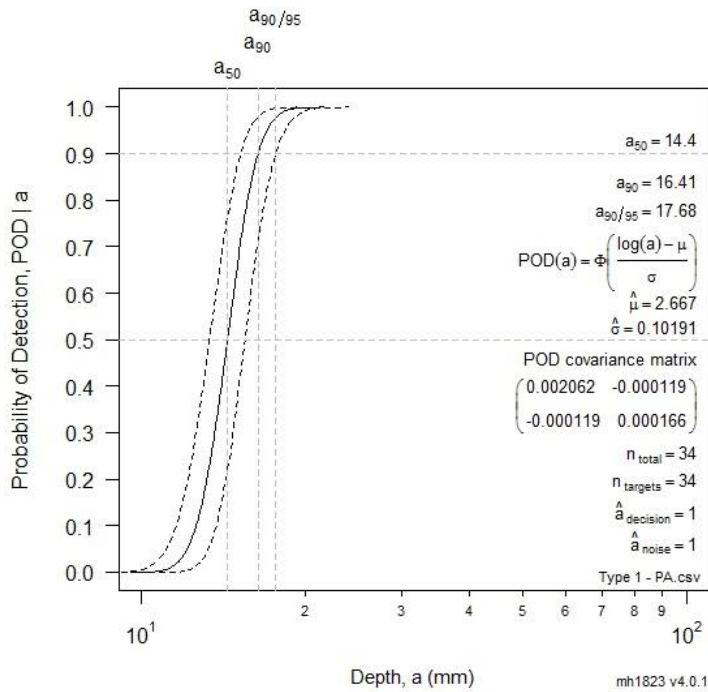


Figure 3.19 PoD curve of Type 1 specimen (PA)

The PoD analysis using depth (a) vs signal response (\hat{a}) data for the ultrasonic and phased array inspection methods are given in Figure 3.18 and 3.19. For ultrasonic testing, the 50 % PoD of flaw (a_{50}) is 28.61 mm in depth. Additionally, 90 % PoD of flaw (a_{90}) is 32.61 mm in depth and 90 % PoD of flaw with a confidence interval of 95 % of a flaw ($a_{90/95}$) depth is 33.41 mm from surface were obtained.

On the other hand, in phased array system, the 50 % PoD of flaw (a_{50}) is 14.4 mm in depth and 90 % PoD of flaw (a_{90}) is 16.41 mm in depth. Finally, 90 % PoD of flaw with a confidence interval of 95 % of a flaw ($a_{90/95}$) depth is 17.68 mm.

Results show that the phased array method is more effective than the ultrasonic method in terms of detecting nearest flaws to the surface. This ability comes from the focal depth property of phased array and also near field disadvantage of ultrasonic testing. Together with above results, the nearest flaw to the surface which is 5 mm in depth, was also determined with phased array system in laboratory tests which couldn't be detected by ultrasonic testing.

3.4 Type 2 Specimen PoD Analysis

3.4.1 Type 2 Specimen (St-37) PoD Analysis

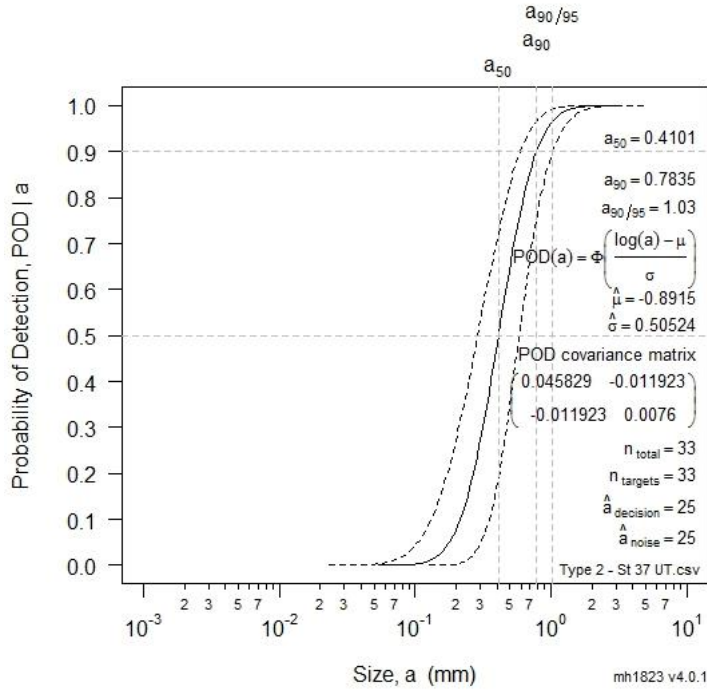


Figure 3.20 PoD curve of Type 2 specimen (St-37 / UT)

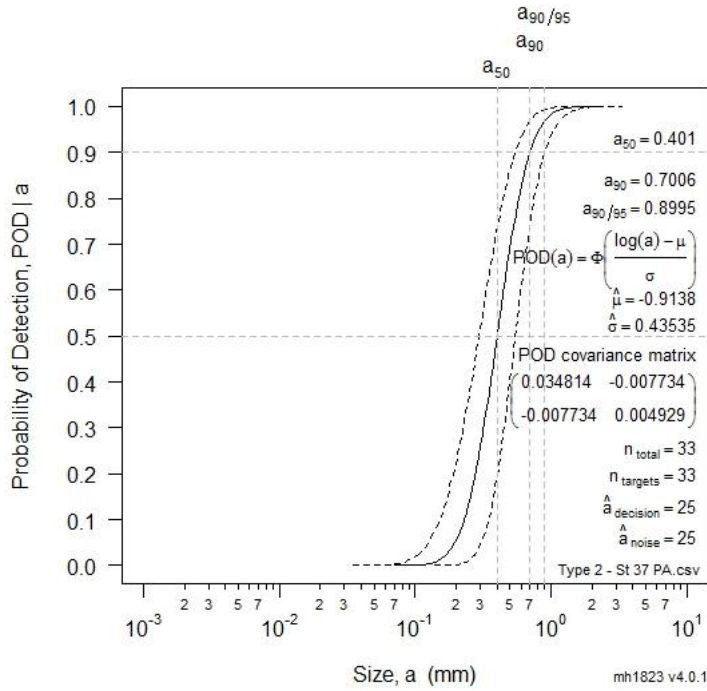


Figure 3.21 PoD curve of Type 2 specimen (St-37 / PA)

Figure 3.20 and 3.21 show that the reliabilities of two inspections systems in terms of flaw sizes do not drastically differ. The 50 % PoD of flaw (a_{50}) is 0.4101 mm in size using ultrasonic testing hence it is 0.401 mm in phased array system. Additionally, 90 % PoD of flaw size (a_{90}) is 0.7835 mm in ultrasonic testing and it is 0.7006 in phased array. Lastly, 90 % PoD of flaw with a confidence interval of 95 % of a flaw ($a_{90/95}$) size is 1.03 in the ultrasonic system and 0.8995 mm in the phased array system. The Phased array system shows a slightly better reliability with comparing ultrasonic system due to its multiple elements which are capable of steer, focus and scan beams with a single probe assembly and depth focusing property.

3.4.2 Type 2 Specimen (SAE 4140) PoD Analysis

Figure 3.22 and 3.23 show that the reliability in terms of PoD approach between two inspection systems do not have significant distinctions.

The 50 % PoD (a_{50}) for the ultrasonic testing is 0.312, for the phased array system, 0.3805. 90 % PoD (a_{90}) is 0.4053 and 0.4714 respectively. 90 % PoD with a confidence interval of 95 % of a flaw ($a_{90/95}$) size is 0.4644 in the ultrasonic system and 0.5296 in the phased array system.

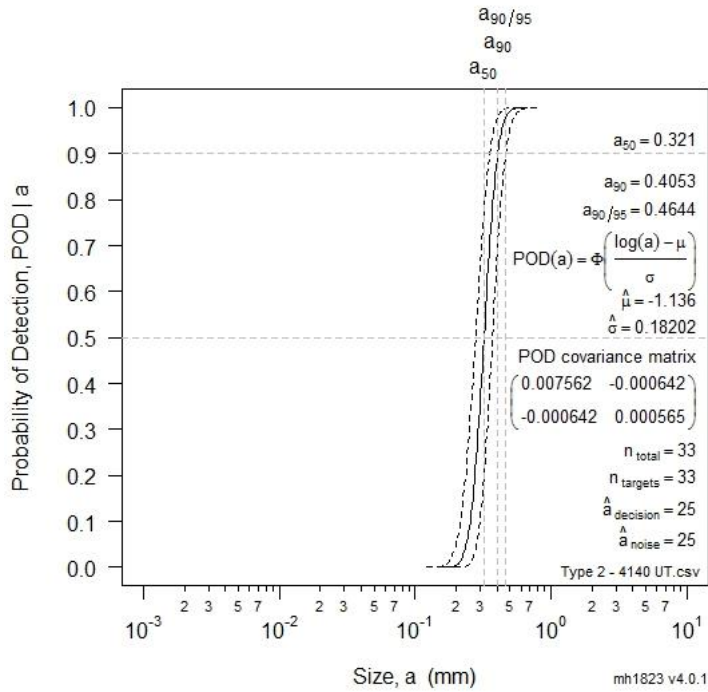


Figure 3.22 PoD curve of Type 2 specimen (SAE 4140 / UT)

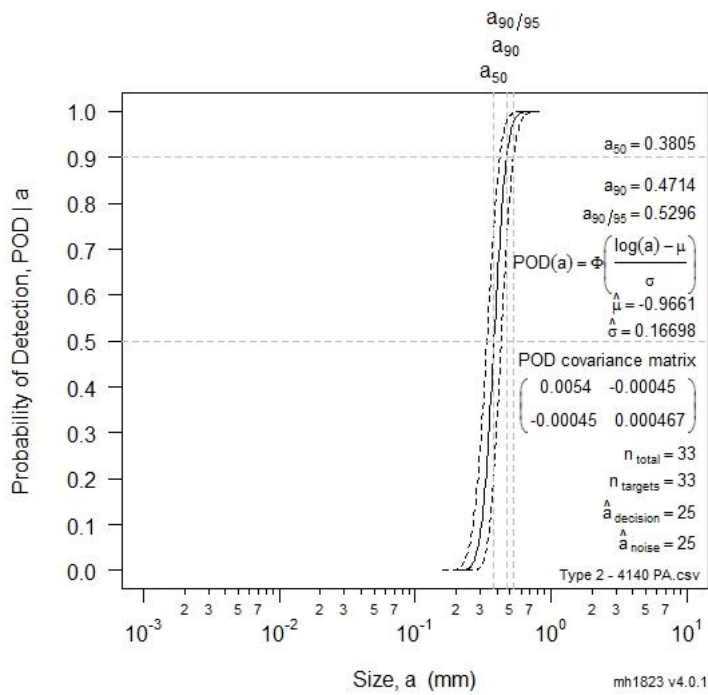


Figure 3.23 PoD curve of Type 2 specimen (SAE 4140 / PA)

3.4.3 Type 2 Specimen (SAE 316) PoD Analysis

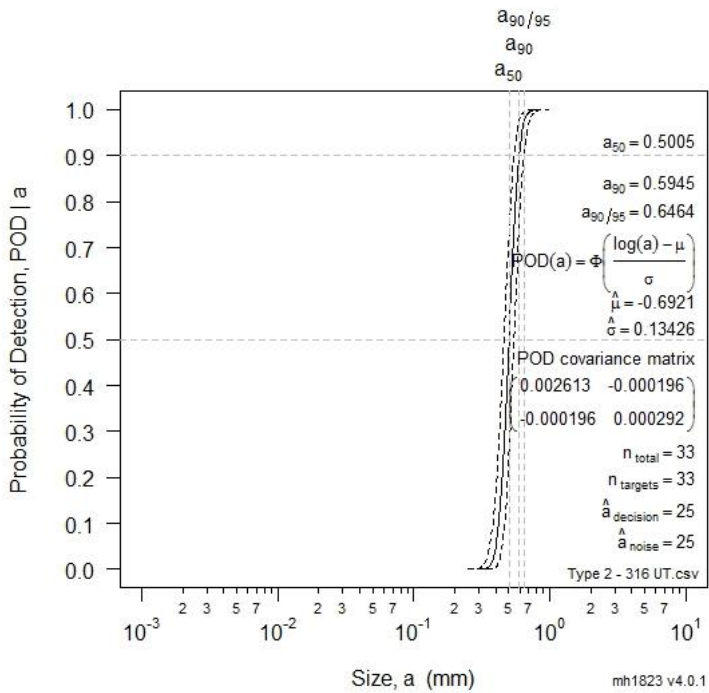


Figure 3.24 PoD curve of Type 2 specimen (SAE 316 L / UT)

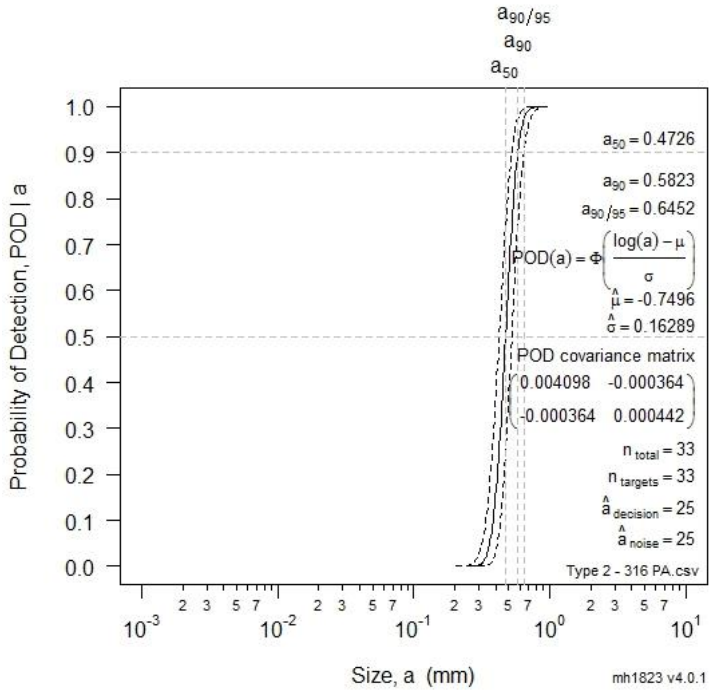


Figure 3.25 PoD curve of Type 2 specimen (SAE 316 L / PA)

PoD curves in SAE 316 L type material given in figure 3.24 and 3.25 show that phased array system reliability in terms of flaw size is slightly better than ultrasonic system.

Flaw sizes are representing 50 % PoD (a_{50}) values for 0.5005 mm in the ultrasonic testing and 0.4726 mm in the phased array system. For projection of 90 % PoD of flaw size (a_{90}), 0.5945 mm and 0.5823 mm are determined respectively. Lastly, 90 % PoD with a confidence interval of 95 % of a flaw ($a_{90,95}$) sizes are 0.6464 in the ultrasonic system and 0.6452 in the phased array system.

The general view for PoD analysis of Type 2 specimen is given in Table 3.1.

Table 3.1 Reliability values for ultrasonic (UT) and phased array (PA) systems

Reliability	St 37		SAE 4140		SAE 316 L	
	UT	PA	UT	PA	UT	PA
50 % PoD	0,41	0,40	0,32	0,38	0,50	0,47
90 % PoD	0,78	0,70	0,41	0,47	0,59	0,58
90 % PoD with a confidence interval of 95 %	1,03	0,90	0,46	0,53	0,65	0,65

The confidence of the system output (reliability of the NDT result) depends on some parameters like, precision, acceptance level and repeatability. But, NDT measurements involve multiple step or multiple element processes that require precision and process control during the execution of each step. There could be some variations in the process which can effect the reliability of system including;

- Material geometry
- Material type
- Artificial flaw characteristic
- Inspection equipment
- Same reference artifacts characteristic
- Inspection equipment

- Inspection procedure and calibration
- Inspection environment

When an NDT process fails to meet expectations, human factors are often cited as the sole causes [26]. As per table 3.1, the negligible differences of results seem to be caused by human factor.

CHAPTER 4

CONCLUSION

The main objective of this thesis is to study the advantages and limitations of phased array system against conventional ultrasonic techniques by using statistical techniques. The comparison between these two methods are modelled by probability of detection (PoD) concept with using two types of steel test blocks containing well-defined artificial defects with different diameters at different depths.

In type 1 specimen, plain carbon steel material was used for inspections. In type 2 specimens, as plain carbon steel St-37, as low-alloyed steel SAE 4140 and as high – alloyed steel SAE 316 L were selected.

PoD analyses were performed using mh1823 software using flaw depth (a) versus signal response, screen height (\hat{a}).

The following conclusions can be drawn from this study:

- In this study, the samples having identical geometries and surface roughness were prepared. Types of materials were selected differently intentionally to see the effect of microstructure on reliability of system. But as far as the PoD values show no devastating differences in this thesis conditions, the effect of material type on reliability seems to be negligible.
- PoD curves shows the superiority of phased array method than conventional ultrasonic testing in determining the nearest flaws to the surface with using

its multiple elements to steer, scan and focus sound beams. For instance, the flaw in 5 mm depth was identified by phased array system due to its focusing ability hence in conventional ultrasonic method, it was missed.

- Same inspection equipment usage in similar environments and calibration process follow-ups decrement the effects of variations of the NDT system. With considering all parameters' alignment for consistent practice makes human factor the reason behind the slight differences in PoD analysis for type 2 specimens.
- In determining the reliability of inspections systems in terms of flaw size, as per the PoD curves, reliabilities of phased array and conventional ultrasonic techniques do not differ significantly under this study's test conditions.
- Microstructure (phases, grain size) of the test specimen do not affect the reliability of test method in this thesis conceptual design. As a result, it can be emphasized that the microstructure of material in this concept is negligible.
- As a further study, in order to monitor the effect of microstructure of test specimen in inspection reliability, artificially created flaws on heat affected zone of the welded samples might be studied.

REFERENCES

- [1] NDT Course Material / Ultrasonic Testing, http://www.ndt-ed.org/EducationResources/CommunityCollege/Ultrasonics/cc_ut_index.htm.
- [2] P. J. Shull, Nondestructive evaluation: theory, techniques, and applications, CRC press, 2002.
- [3] J. R. Davis, ASM Handbook: Nondestructive evaluation and quality control, in: vol 17, ASM International, 1989, pp. 487 - 490.
- [4] P. He, Direct measurement of ultrasonic dispersion using a broadband transmission technique, Ultrasonics, 1999, p. 67-70.
- [5] C. H. Gür, B. Aydinmakina, Ultrasonic investigation of graphite nodularity in ductile cast irons, Journal of Nondestructive Testing & Ultrasonic (Germany), vol 7, 2002, p. 7.
- [6] R. Raisutis, R. Kazys, A. Voleisis, Application of the through transmission ultrasonic technique for estimation of the phase velocity dispersion in plastic materials, Ultrasound, vol. 63, 2008, pp. 15-18.
- [7] Phased Array Testing: Basic Theory for Industrial Applications, Olympus NDT, 2012.
- [8] T. Armitt, Phased arrays not the answer to every application, Non Destructive Testing Australia, vol. 43, 2006, p. 189.
- [9] M. D. Nel, Ultrasonic Phased Arrays: An Insight into an Emerging Technology, in: Proceedings National Seminar on Non-Destructive Evaluation, 2006.
- [10] Advances in Phased Array Ultrasonic Technology Applications, Olympus NDT, 2007.
- [11] Phased Array Technology, http://www.nde.com/phased_array_technology.htm.
- [12] Introduction to Phased Array Ultrasonic Technology Applications: R/D tech guideline, Olympus NDT, 2007.
- [13] M. Jobst, G. D. Connolly, Demonstration of the application of the total focusing method to the inspection of steel welds, 10th European Conference on NDT, 2010.

- [14] C. Schneider, C. Twi, B. England Colin, D. Babcock, Reliability of manually applied phased array inspection, 4th European-American Workshop on Reliability of NDE, 2009.
- [15] P. Ciorau, Contribution to detection and sizing linear defects by conventional and phased array ultrasonic techniques, *Journal of Nondestructive Testing*, vol 10, 2005.
- [16] M. Moles, Portable phased array applications, *Non Destructive Testing Australia*, vol 45, 2008, p. 88.
- [17] M. Moles, NDT Olympus, Manual phased arrays for weld inspections using North American codes, *Abstracts of 17th World Conference on Non-Destructive Testing*, 2008.
- [18] G. Persson, H. Wirdelius, P. Hammersberg, Synthetic Non-Parametric POD for Large Defects, *18th World Conference on Nondestructive Testing*, 2012, pp. 16-20.
- [19] W. D. Rummel, G. A. Matzkanin, *Nondestructive Evaluation Capabilities Data Book*, NTIAC: DB-97-02, Nondestructive Testing Information Analysis Center (NTIAC), 1997.
- [20] G. A. Georgiou, Probability of Detection (POD) curves: derivation, applications and limitations, *Jacobi Consulting Limited Health and Safety Executive Research Report*, vol 454, 2006.
- [21] F. R. Child, D. H. Phillips, L. W. Liese, W. D. Rummel, Quantitative Assessment of the Detectability of Ceramic Inclusions in Structural Titanium Castings by X-Radiography, *Review of Progress in Quantitative Nondestructive Evaluation*, Springer, 1999, pp. 2311-2317.
- [22] C. Müller, M. Elaguine, C. Bellon, U. Ewert, U. Zscherpel, M. Scharmach, B. Redmer, H. Ryden, U. Ronneteg, POD (Probability of Detection) Evaluation of NDT Techniques for Cu-Canisters for Risk Assessment of Nuclear Waste Encapsulation, *Proceedings of the 9th European Conference on NDT*, 2006, pp. 25-29.
- [23] J. Rudlin, W. D. Dover, Results of probability of detection trials, *Proceedings of International Offshore Contracting & Subsea Engineering*, 1992, pp. 13-16.

- [24] J. H. Kurz, A. Jüngert, S. Dugan, G. Dobmann, Probability of Detection (POD) determination using ultrasound phased array for considering NDT in probabilistic damage assessments, 18th World Conference on Nondestructive Testing, 2012.
- [25] ASTM, E2862-12 Standard Practice for Probability of Detection analysis for Hit/Miss Data, 2012.
- [26] W. D. Rummel, Probability of Detection as a quantitative measure of nondestructive testing end-to-end process capabilities, *Materials Evaluation*, vol 56, 1998.
- [27] J. R. Davis, *ASM Handbook: Nondestructive evaluation and quality control*, ASM International, vol 17, 1989, pp. 1438-1449.
- [28] M. Li, New methods for statistical modeling and analysis of nondestructive evaluation data, *Statistics*, Iowa State University, PhD. Thesis, Iowa, 2010.
- [29] A. P. Berens, P. W. Hovey, Evaluation of NDE reliability characterization, Defense Technical Information Center, 1981.
- [30] M. Pavlovic, K. Takahashi, C. Müller, R. Boehm, U. Ronneteg, Reliability in Non-Destructive Testing (NDT) of the Canister Components. NDT Reliability Final Report, SKB Technical report R-08-129, Swedish Nuclear Fuel and Waste Management Co, 2008.
- [31] C. Annis, MIL-HDBK-1823A, Nondestructive Evaluation System Reliability Assessment, 2009.
- [32] M. Spies, H. Rieder, Enhancement of PoD Flaws in the Bulk of Highly Attenuating Structural Materials by Using SAFT Processed Ultrasonic Inspection Data, *Materials Testing*, vol. 52, 2009, pp. 160-165.
- [33] S. Kierspel, T. Ballanger, M. Berke, Is There Really Any Value to Multiple Angle Manual Inspection?, Asia-Pacific Conference on NDT, 2006.
- [34] J. Haapalainen, E. Leskela, Probability of detection simulations for ultrasonic pulse-echo testing, Proceedings of 18th World Conference on Nondestructive Testing, Durban, South Africa, 2012.
- [35] U. Isleyici, Effect of Surface Roughness on Ultrasonic Testing, Mechanical Engineering, Middle East Technical University, MSc. Thesis, Ankara, 2005.
- [36] Carbon steel, http://en.wikipedia.org/wiki/Carbon_steel.

- [37] EN, 10025--2 Hot Rolled Products of Structural Steels-Part 2: Technical Delivery Condition for Non-Alloy Structural Steel, 2004.
- [38] F. S. William, J. Hashemi, Foundations of materials science and engineering, Mcgraw-Hill Publishing, 2006.
- [39] S. D. Washko, G. Aggen, Wrought stainless steels, ASM International, Metals Handbook. Tenth Edition., 1990, p. 841-907.
- [40] S. Kalpajian, S. R. Schmid, Material removal processes: abrasive, chemical, electrical and high-energy beam. Manufacturing processes for engineering materials, Prentice Hall, 2003, p. 541.
- [41] K. H. Ho, S. T. Newman, State of the art electrical discharge machining (EDM), International Journal of Machine Tools and Manufacture, 2003, p. 1287-1300.
- [42] P. P. Nanekar, B. K. Shah, Characterization of material properties by ultrasonics, National Seminar on Non-Destructive Evaluation, 2003.
- [43] C. H. Gür, B. O. Tuncer, Investigating the microstructure-ultrasonic property relationships in steels, 16th WCNDT-World Conference on NDT, 2004.
- [44] C. Annis, Statistical Best-Practices for Building Probability of Detection (POD) models, R package mh1823, version 4.0.1, <http://StatisticalEngineering.com/mh1823/>, 2014.